

required for H4 acetylation; indeed, the most effective dose of SB in HD mouse study, 1200 mg/kg/day, was higher than that in our analysis, 800–900 mg/kg/day.

We have previously described therapeutic approaches for SBMA using our Tg mouse model (45). Reduction in the testosterone level by castration or leuprorelin administration diminished nuclear-localized mutant AR and markedly prevented phenotypic expression in the male Tg mice (17,18). Overexpression of heat shock protein 70, which is a molecular chaperone refolding mutant protein (46), resulted in acceleration of mutant AR degradation and phenotypic amelioration (19). Although these strategies show therapeutic promise, single therapeutic agents possess limited potential because of their side effects. As suggested for other neurodegenerative diseases (47), combinations of drugs appear to be useful in the attempts of obtaining maximal therapeutic effects and reducing harmful events. Although the exact mechanism remains to be clarified, SB also ameliorates neuromuscular phenotypes of spinal muscular atrophy, which is another lower motor neuron disease arising from a different gene mutation (48). This result might indicate the relatively potent effects of SB on affected lower motor neurons. SB is a promising candidate for combination therapy for SBMA, although its dose should be very carefully determined for clinical use.

MATERIALS AND METHODS

Generation and maintenance of Tg mice and genotyping

Chicken β -actin promoter-driven AR-24Q and AR-97Q constructs were prepared by digestion of pCAGGS vector as described earlier (17,49,50). Genotyping of mice was performed by PCR using mouse tail (17). Tg mice were maintained by crossing to F1 of C57BL/6J and BDF1. We analyzed a symptomatic line #4–6 of this mouse model throughout the present study.

Assessment of motor ability

All animal experiments were performed in accordance with the National Institute of Health Guide for the Care and Use of Laboratory Animals and were approved by the Nagoya University Animal Experiment Committee. Rotarod performance was assessed weekly using an Economex Rotarod (Colombus Instruments, Columbus, OH, USA) as described previously (51). Cage activity was measured weekly, with each mouse in a transparent acrylic cage within a soundproof box as described previously (17).

Administration of SB

Wt and SBMA Tg (AR-97Q #4–6) mice were orally supplied sterile water *ad libitum*. Three mice shared the same drinking water in each cage. SB was administered at a concentration of 2, 4, 8, 16 or 40 g/l in distilled water from 5 weeks of age until the end of analysis. Before the onset of motor symptoms, between the age of 6 and 8 weeks, the approximate daily amount of drinking water was similar for each treatment group of Tg mice; 4.0 ± 0.26 , 3.7 ± 0.51 , 4.5 ± 0.19 ,

4.1 ± 0.29 and 4.4 ± 0.15 ml at the dose of 0, 2, 4, 8 and 16 g/l, respectively. There was no difference in the amount of water intake and body weight between Wt and Tg mice in that period.

Immunohistochemistry

An aliquot of 20 ml of 4% paraformaldehyde fixative in 0.1 M phosphate buffer (pH 7.4) was perfused through the left cardiac ventricle of mice (12 weeks old) deeply anesthetized with ketamine–xylazine, the tissues post-fixed in 10% phosphate-buffered formalin and then processed for paraffin embedding. Tissue sections (4 μ m thick) were then deparaffinized, dehydrated with alcohol, and then treated for antigen retrieval (17). For the mutant AR immunohistochemical study, the paraffin sections were pretreated with formic acid for 5 min at room temperature. The tissue sections were blocked with normal horse serum (1:20) and incubated with mouse anti-expanded polyQ, 1C2 (1:10 000, Chemicon, Temecula, CA, USA). The sections were then incubated with biotinylated anti-mouse IgG (1:1000, Vector Laboratories, Burlingame, CA, USA). Immune complexes were visualized using streptavidin–horseradish peroxidase (Dako, Glostrup, Denmark) and 3,3'-diaminobenzidine (Dojindo, Kumamoto, Japan) substrate. Sections were counterstained with methyl green. For immunostaining of histone, sections were autoclaved at 121°C for 15 min, and incubated with anti-histone H3 (1:100, Upstate Biotechnology, Lake Placid, NY, USA) or anti-acetylated histone H3 (1:500, Upstate Biotechnology) antibodies.

The number of 1C2 or anti-acetylated H3-positive cells for one individual mouse was counted using a light microscope with a computer-assisted image analyzer (Luzex FS, Nikon, Tokyo, Japan). Fifty consecutive transverse sections of the thoracic spinal cord were prepared, and 1C2 or anti-acetylated H3-positive cells in the anterior horn on every fifth section were counted as described previously (51,52). For quantitative assessment, 1C2-positive cells in the muscle were calculated from counts of more than 500 fibers in randomly selected areas, and were expressed as the number per 100 muscle fibers.

Muscle histology and morphometric analysis of spinal motor neurons and ventral spinal roots

Cryostat sections of the gastrocnemius muscles (6 μ m thick) were air-dried and stained with hematoxylin and eosin (H&E). The muscle fiber diameter was measured in randomly selected areas for three mice of each treatment group (12 weeks old) using a Luzex FS image analyzer (Nireco). To assess the neuronal populations and cross-sectional area of the anterior horn cells, 20 serial 5 μ m thick sections from the fifth lumbar spinal cords of three mice of each group (12 weeks old) were prepared. Every other section was stained by the Nissl technique, and all neurons with an obvious nucleolus in the anterior horn were assessed using a Luzex FS image analyzer as described earlier (17). The diameter of myelinated fibers in the ventral spinal roots was measured on the transverse sections stained with toluidine blue, also as described earlier (17).

Western blots

Mice (12 weeks old) were exsanguinated under ketamine–xylazine anesthesia, and their tissues snap-frozen with powdered CO₂ in acetone. Frozen tissue (0.1 g wet weight) was homogenized in 1000 µl of CelLytic-M mammalian cell lysis/extraction reagent (Sigma Chemical, St Louis, MO, USA) with 1 mM phenylmethylsulfonyl fluoride and aprotinin at 6 µg/ml. Homogenates were spun at 2500g for 15 min at 4°C. The protein concentration of the supernatant was determined using DC protein assay (Bio-Rad Laboratories, Hercules, CA, USA). Each lane on a 5–20% SDS–PAGE gel was loaded with 200 µg protein for the spinal cord and 80 µg for the muscle from the supernatant fraction, which was transferred to Hybond-P membranes (Amersham Pharmacia Biotech, Buckinghamshire, UK) using 25 mM Tris, 192 mM glycine and 10% methanol as transfer buffer. Kaleidoscope prestained standards were used as size markers (Bio-Rad Laboratories). Proteins were then transferred to Hybond-P membranes (Amersham Pharmacia Biotech), which were subsequently blocked in 5% milk in Tris-buffered saline containing 0.05% Tween-20, and incubated with appropriate primary antibodies using standard techniques. Primary antibodies were used at the following concentrations: anti-histone H3, 1:500 (Upstate Biotechnology); anti-acetylated histone H3, 1:250 (Upstate Biotechnology); anti-histone H4, 1:500 (Upstate Biotechnology); anti-acetylated histone H4, 1:200 (Upstate Biotechnology); anti-histone H2A, 1:500 (Upstate Biotechnology); anti-acetylated histone H2A, 1:200 (Upstate Biotechnology); anti-histone H2B, 1:500 (Upstate Biotechnology) and anti-acetylated histone H2B, 1:200 (Serotec, Kidlington, UK). Second antibody probing and detection were performed using the ECL + plus kit (Amersham Pharmacia Biotech) as described earlier (17). The signal intensity of the bands smearing from the top of the gel were quantified using the NIH Image program (NIH Image version 1.62). The quantitative data of three independent western blots were expressed as mean ± SD.

Statistical analyses

Data were analyzed using Kaplan–Meier and log-rank test for survival rate in Figure 2, Dunnett test for multiple comparison in Figures 3A–C and 6B and unpaired *t*-test in Figures 4, 5 and 6D from Statview software version 5 (HULINKS, Tokyo, Japan).

ACKNOWLEDGEMENTS

We thank Dr Tamakoshi and Dr Yatsuya for their advice in the statistical analysis. This work was supported by a Center-of-Excellence (COE) grant from the Ministry of Education, Culture, Sports, Science and Technology, Japan, grants from the Ministry of Health, Labor and Welfare, Japan, a grant from the Naito Foundation and a grant from the Kanae Foundation.

REFERENCES

- Zoghbi, H.Y. and Orr, H.T. (2000) Glutamine repeats and neurodegeneration. *Annu. Rev. Neurosci.*, **23**, 217–247.

- Ross, C.A. (2002) Polyglutamine pathogenesis: emergence of unifying mechanisms for Huntington's disease and related disorders. *Neuron*, **35**, 819–822.
- Margolis, R.L. and Ross, C.A. (2002) Expansion explosion: new clues to the pathogenesis of repeat expansion neurodegenerative diseases. *Trends. Mol. Med.*, **7**, 479–482.
- Kennedy, W.R., Alter, M. and Sung, J.H. (1968) Progressive proximal spinal and bulbar muscular atrophy of late onset. A sex-linked recessive trait. *Neurology*, **18**, 671–680.
- Sobue, G., Hashizume, Y., Mukai, E., Hirayama, M., Mitsuma, T. and Takahashi, A. (1989) X-linked recessive bulbospinal neuronopathy. A clinicopathological study. *Brain*, **112**, 209–232.
- Takahashi, A. (2001) Hiroshi Kawahara (1858–1918). *J. Neurol.*, **248**, 241–242.
- La Spada, A.R., Wilson, E.M., Lubahn, D.B., Harding, A.E. and Fischbeck, K.H. (1991) Androgen receptor gene mutations in X-linked spinal and bulbar muscular atrophy. *Nature*, **352**, 77–79.
- Tanaka, F., Doyu, M., Ito, Y., Matsumoto, M., Mitsuma, T., Abe, K., Aoki, M., Itoyama, Y., Fischbeck, K.H. and Sobue, G. (1996) Founder effect in spinal and bulbar muscular atrophy (SBMA). *Hum. Mol. Genet.*, **5**, 1253–1257.
- Tanaka, F., Reeves, M.F., Ito, Y., Matsumoto, M., Li, M., Miwa, S., Inukai, A., Yamamoto, M., Doyu, M., Yoshida, M. *et al.* (1999) Tissue-specific somatic mosaicism in spinal and bulbar muscular atrophy is dependent on CAG-repeat length and androgen receptor–gene expression level. *Am. J. Hum. Genet.*, **65**, 966–973.
- Doyu, M., Sobue, G., Mukai, E., Kachi, T., Yasuda, T., Mitsuma, T. and Takahashi, A. (1992) Severity of X-linked recessive bulbospinal neuronopathy correlates with size of the tandem CAG repeat in androgen receptor gene. *Ann. Neurol.*, **23**, 707–710.
- La Spada, A.R., Roling, D.B., Harding, A.E., Warner, C.L., Spiegel, R., Hausmanowa-Petrusewicz, L., Yee, W.C. and Fischbeck, K.H. (1992) Meiotic stability and genotype-phenotype correlation of the trinucleotide repeat in X-linked spinal and bulbar muscular atrophy. *Nat. Genet.*, **2**, 301–304.
- Igarashi, S., Tanno, Y., Onodera, O., Yamazaki, M., Sato, S., Ishikawa, A., Miyatani, N., Nagashima, M., Ishikawa, Y., Sahashi, K. *et al.* (1992) Strong correlation between the number of CAG repeats in androgen receptor genes and the clinical onset of features of spinal and bulbar muscular atrophy. *Neurology*, **42**, 2300–2302.
- Li, M., Miwa, S., Kobayashi, Y., Merry, D.E., Tanaka, F., Doyu, M., Hashizume, Y., Fischbeck, K.H. and Sobue, G. (1998) Nuclear inclusions of the androgen receptor protein in spinal and bulbar muscular atrophy. *Ann. Neurol.*, **44**, 249–254.
- Li, M., Nakagomi, Y., Kobayashi, Y., Merry, D.E., Tanaka, F., Doyu, M., Mitsuma, T., Fischbeck, K.H. and Sobue, G. (1998) Nonneural nuclear inclusions of androgen receptor protein in spinal and bulbar muscular atrophy. *Am. J. Pathol.*, **153**, 695–701.
- Tobin, A.J. and Signer, E.R. (2000) Huntington's disease: the challenge for cell biologists. *Trends Cell Biol.*, **10**, 531–536.
- Taylor, J.P., Hardy, J. and Fischbeck, K.H. (2002) Toxic proteins in neurodegenerative disease. *Science*, **296**, 1991–1995.
- Katsuno, M., Adachi, H., Kume, A., Li, M., Nakagomi, Y., Niwa, H., Sang, C., Kobayashi, Y., Doyu, M. and Sobue, G. (2002) Testosterone reduction prevents phenotypic expression in a transgenic mouse model of spinal and bulbar muscular atrophy. *Neuron*, **35**, 843–854.
- Katsuno, M., Adachi, H., Doyu, M., Minamiyama, M., Sang, C., Kobayashi, Y., Inukai, A. and Sobue, G. (2003) Leuporelin rescues polyglutamine-dependent phenotypes in a transgenic mouse model of spinal and bulbar muscular atrophy. *Nat. Med.*, **9**, 768–773.
- Adachi, H., Katsuno, M., Minamiyama, M., Sang, C., Pagoulatos, G., Angelidis, C., Kusakabe, M., Yoshiki, A., Kobayashi, Y., Doyu, M. *et al.* (2003) Heat shock protein 70 chaperone overexpression ameliorates phenotypes of the spinal and bulbar muscular atrophy transgenic mouse model by reducing nuclear-localized mutant androgen receptor protein. *J. Neurosci.*, **23**, 2203–2211.
- McC Campbell, A., Taylor, J.P., Taye, A.A., Robitschek, J., Li, M., Walcott, J., Merry, D., Chai, Y., Paulson, H., Sobue, G. *et al.* (2000) CREB-binding protein sequestration by expanded polyglutamine. *Hum. Mol. Genet.*, **9**, 2197–2202.
- Nucifora, F.C. Jr, Sasaki, M., Peters, M.F., Huang, H., Cooper, J.K., Yamada, M., Takahashi, H., Tsuji, S., Troncoso, J., Dawson, V.L. *et al.*

- (2001) Interference by huntingtin and atrophin-1 with CBP-mediated transcription leading to cellular toxicity. *Science*, **291**, 2423–2428.
22. Steffan, J.S., Kazantsev, A., Spasic-Boskovic, O., Greenwald, M., Zhu, Y.Z., Gohler, H., Wanker, E.E., Bates, G.P., Housman, D.E. and Thompson, L.M. (2000) The Huntington's disease protein interacts with p53 and CREB-binding protein and represses transcription. *Proc. Natl Acad. Sci. USA*, **97**, 6763–6768.
 23. Dunah, A.W., Jeong, H., Griffin, A., Kim, Y.M., Standaert, D.G., Hersch, S.M., Mouradian, M.M., Young, A.B., Tanese, N. and Krainc, D. (2002) Sp1 and TAFII130 transcriptional activity disrupted in early Huntington's disease. *Science*, **296**, 2238–2243.
 24. Steffan, J.S., Bodai, L., Pallos, J., Poelman, M., McCampbell, A., Apostol, B.L., Kazantsev, A., Schmidt, E., Zhu, Y.Z., Greenwald, M. *et al.* (2001) Histone deacetylase inhibitors arrest polyglutamine-dependent neurodegeneration in *Drosophila*. *Nature*, **413**, 739–743.
 25. McCampbell, A., Taye, A.A., Whitty, L., Penney, E., Steffan, J.S. and Fischbeck, K.H. (2001) Histone deacetylase inhibitors reduce polyglutamine toxicity. *Proc. Natl Acad. Sci. USA*, **98**, 15179–15184.
 26. Hockly, E., Richon, V.M., Woodman, B., Smith, D.L., Zhou, X., Rosa, E., Sathasivam, K., Ghazi-Noori, S., Mahal, A., Lowden, P.A. *et al.* (2003) Suberoylanilide hydroxamic acid, a histone deacetylase inhibitor, ameliorates motor deficits in a mouse model of Huntington's disease. *Proc. Natl Acad. Sci. USA*, **100**, 2041–2046.
 27. Cha, J.H. (2000) Transcriptional dysregulation in Huntington's disease. *Trends Neurosci.*, **23**, 387–392.
 28. Sugars, K.L. and Rubinsztein, D.C. (2003) Transcriptional abnormalities in Huntington disease. *Trends Genet.*, **19**, 233–238.
 29. Bates, G. (2003) Huntingtin aggregation and toxicity in Huntington's disease. *Lancet*, **361**, 1642–1644.
 30. Sanchez, I., Mahlke, C. and Yuan, J. (2003) Pivotal role of oligomerization in expanded polyglutamine neurodegenerative disorders. *Nature*, **421**, 373–379.
 31. Kobayashi, Y., Miwa, S., Merry, D.E., Kume, A., Mei, L., Doyu, M. and Sobue, G. (1998) Caspase-3 cleaves the expanded androgen receptor protein of spinal and bulbar muscular atrophy in a polyglutamine repeat length-dependent manner. *Biochem. Biophys. Res. Commun.*, **252**, 145–150.
 32. Karpuj, M.V., Becher, M.W., Springer, J.E., Chabas, D., Youssef, S., Pedotti, R., Mitchell, D. and Steinman, L. (2002) Prolonged survival and decreased abnormal movements in transgenic model of Huntington disease, with administration of the transglutaminase inhibitor cystamine. *Nat. Med.*, **8**, 143–149.
 33. Panov, A.V., Gutekunst, C.A., Leavitt, B.R., Hayden, M.R., Burke, J.R., Strittmatter, W.J. and Greenamyre, J.T. (2002) Early mitochondrial calcium defects in Huntington's disease are a direct effect of polyglutamines. *Nat. Neurosci.*, **5**, 731–736.
 34. La Spada, A.R. and Taylor, J.P. (2003) Polyglutamines placed into context. *Neuron*, **38**, 681–684.
 35. Lin, X., Antalffy, B., Kang, D., Orr, H.T. and Zoghbi, H.Y. (2000) Polyglutamine expansion down-regulates specific neuronal genes before pathologic changes in SCA1. *Nat. Neurosci.*, **3**, 157–163.
 36. Luthi-Carter, R., Strand, A., Peters, N.L., Solano, S.M., Hollingsworth, Z.R., Menon, A.S., Frey, A.S., Spector, B.S., Penney, E.B., Schilling, G. *et al.* (2000) Decreased expression of striatal signaling genes in a mouse model of Huntington's disease. *Hum. Mol. Genet.*, **9**, 1259–1271.
 37. Wyttenbach, A., Swartz, J., Kita, H., Thykjaer, T., Carmichael, J., Bradley, J., Brown, R., Maxwell, M., Schapira, A., Orntoft, T.F. *et al.* (2001) Polyglutamine expansions cause decreased CRE-mediated transcription and early gene expression changes prior to cell death in an inducible cell model of Huntington's disease. *Hum. Mol. Genet.*, **10**, 1829–1845.
 38. Kita, H., Carmichael, J., Swartz, J., Muro, S., Wyttenbach, A., Matsubara, K., Rubinsztein, D.C. and Kato, K. (2002) Modulation of polyglutamine-induced cell death by genes identified by expression profiling. *Hum. Mol. Genet.*, **11**, 2279–2287.
 39. Ferrante, R.J., Kubilus, J.K., Lee, J., Ryu, H., Beesen, A., Zucker, B., Smith, K., Kowall, N.W., Ratan, R.R., Luthi-Carter, R. and Hersch, S.M. (2003) Histone deacetylase inhibition by sodium butyrate chemotherapy ameliorates the neurodegenerative phenotype in Huntington's disease mice. *J. Neurosci.*, **23**, 9418–9427.
 40. McCampbell, A. and Fischbeck, K.H. (2001) Polyglutamine and CBP: fatal attraction? *Nat. Med.*, **7**, 528–530.
 41. Kramer, O.H., Gottlicher, M. and Heinzel, T. (2001) Histone deacetylase as a therapeutic target. *Trends Endocrinol. Metab.*, **12**, 294–300.
 42. Kelly, W.K., Richon, V.M., O'Connor, O., Curley, T., MacGregor-Curtelli, B., Tong, W., Klang, M., Schwartz, L., Richardson, S., Rosa, E. *et al.* (2003) Phase I clinical trial of histone deacetylase inhibitor: suberoylanilide hydroxamic acid administered intravenously. *Clin. Cancer Res.*, **9**, 3578–3588.
 43. Carducci, M.A., Gilbert, J., Bowling, M.K., Noe, D., Eisenberger, M.A., Sinibaldi, V., Zabelina, Y., Chen, T.L., Grochow, L.B. and Donehower, R.C. (2001) A phase I clinical and pharmacological evaluation of sodium phenylbutyrate on a 120-h infusion schedule. *Clin. Cancer Res.*, **7**, 3047–3055.
 44. Egorin, M.J., Yuan, Z.M., Sentz, D.L., Plaisance, K. and Eiseman, J.L. (1999) Plasma pharmacokinetics of butyrate after intravenous administration of sodium butyrate or oral administration of tributyrin or sodium butyrate to mice and rats. *Cancer Chemother. Pharmacol.*, **43**, 445–453.
 45. Katsuno, M., Adachi, H., Inukai, A. and Sobue, G. (2003) Transgenic mouse models of spinal and bulbar muscular atrophy (SBMA). *Cytogenet. Genome Res.*, **100**, 243–251.
 46. Kobayashi, Y. and Sobue, G. (2001) Protective effect of chaperones on polyglutamine diseases. *Brain Res. Bull.*, **56**, 165–168.
 47. Kriz, J., Gowing, G. and Julien, J.P. (2003) Efficient three-drug cocktail for disease induced by mutant superoxide dismutase. *Ann. Neurol.*, **53**, 429–436.
 48. Chang, J.G., Hsieh-Li, H.M., Jong, Y.J., Wang, N.M., Tsai, C.H. and Li, H. (2001) Treatment of spinal muscular atrophy by sodium butyrate. *Proc. Natl Acad. Sci. USA*, **98**, 9808–9813.
 49. Niwa, H., Yamamura, K. and Miyazaki, J. (1991). Efficient selection for high-expression transfectants with a novel eukaryotic vector. *Gene*, **108**, 193–199.
 50. Kobayashi, Y., Kume, A., Li, M., Doyu, M., Hata, M., Ohtsuka, K. and Sobue, G. (2000) Chaperones Hsp70 and Hsp40 suppress aggregate formation and apoptosis in cultured neuronal cells expressing truncated androgen receptor protein with expanded polyglutamine tract. *J. Biol. Chem.*, **275**, 8772–8778.
 51. Adachi, H., Kume, A., Li, M., Nakagomi, Y., Niwa, H., Do, J., Sang, C., Kobayashi, Y., Doyu, M. and Sobue, G. (2001) Transgenic mice with an expanded CAG repeat controlled by the human AR promoter show polyglutamine nuclear inclusions and neuronal dysfunction without neuronal cell death. *Hum. Mol. Genet.*, **10**, 1039–1048.
 52. Terao, S., Sobue, G., Hashizume, Y., Li, M., Inagaki, T. and Mitsuma, T. (1996). Age-related changes in human spinal ventral horn cells with special reference to the loss of small neurons in the intermediate zone: a quantitative analysis. *Acta Neuropathol.*, **92**, 109–114.

Polyglutamine Diminishes VEGF: Passage to Motor Neuron Death?

Altered gene transcription has been implicated in the pathogenesis of polyglutamine-dependent neurodegeneration. In this issue of *Neuron*, Sopher et al. demonstrate that androgen receptors containing expanded polyglutamine cause decreased expression of vascular endothelial growth factor (VEGF) by interfering with cAMP response element binding protein binding protein (CBP), thereby contributing to the motor neuron degeneration in spinal and bulbar muscular atrophy.

Expansion of a triplet nucleotide repeat is the molecular basis for a variety of hereditary neuromuscular diseases. At least nine neurodegenerative diseases result from a tedious trinucleotide CAG repeat, which encodes a polyglutamine tract (reviewed in Zoghbi and Orr, 2000). These disorders, called polyglutamine diseases, include spinal and bulbar muscular atrophy (SBMA), Huntington's disease (HD), spinocerebellar ataxias (SCA1, 2, 3, 6, 7, and 17), and dentatorubral pallidoluysian atrophy (DRPLA). Several shared clinical and histopathological features seen in polyglutamine diseases imply a common pathogenesis. The patients suffer from slow progressive neuromuscular symptoms with the onset in adulthood. Although the causative genes are distinct, selected subsets of neurons in the central nervous system undergo degeneration in each disease. Histopathological hallmarks are the loss of neurons in the affected area and the existence of characteristic intranuclear inclusions in the residual neuronal cells. These inclusions contain aggregates of the causative protein together with fundamental cellular components, providing a clue to the mechanisms causing neurodegeneration. Although the precise role of these inclusions remains open to debate, a large body of evidence suggests that the nuclear localization of aberrant polyglutamine protein is an essential step in the pathogenesis.

The perturbation of gene transcription is likely to be among the most substantial nuclear events in the pathophysiology of polyglutamine diseases. This hypothesis emerged from the observation that cAMP response element binding protein binding protein (CBP), a transcriptional coactivator, is sequestered into the polyglutamine inclusion (Nucifora et al., 2001). Furthermore, the acetyltransferase activity of CBP is directly inhibited by the interaction with aberrant polyglutamine protein (Steffan et al., 2001). In agreement with these findings, alteration of a wide range of gene expression has been detected in mouse models of polyglutamine diseases (Sugars and Rubinsztein, 2003). It is of therapeutic significance that polyglutamine-mediated neurodegeneration in a *Drosophila* model of HD is alleviated by histone

deacetylase inhibitors, which restore histone acetylation and upregulate gene transcriptions (Steffan et al., 2001). Although decreased transcription appears to be a plausible explanation for the pathogenesis, little direct link between CBP dysfunction and neurodegeneration has been clarified *in vivo*. In addition, it remains unclear which gene is responsible for neuronal cell death in each polyglutamine disease.

Spinal and bulbar muscular atrophy (SBMA), or Kennedy's disease, which is caused by an expanded CAG repeat in the androgen receptor (AR) gene, was the first disease to be identified as a polyglutamine disease (La Spada et al., 1991). SBMA is an adult-onset lower motor neuron disease characterized by proximal muscle atrophy, weakness, fasciculations, and bulbar involvement. In the central nervous system, the brainstem and the anterior horn are selectively involved. Besides motor neuron degeneration, patients present with several systemic complications: gynecomastia, hyperlipidemia, and glucose intolerance. Since the loss of AR function does not result in neuromuscular phenotypes, the extended polyglutamine tract itself appears to render the causative protein toxic, as documented in other polyglutamine diseases. The disruption of CBP-mediated transcription has also been implicated in the pathogenesis of this disease (McCampbell et al., 2001). Despite a common molecular basis, SBMA is distinct from other polyglutamine diseases in that males are exclusively affected. A transgenic mouse model of SBMA revealed that ligand-dependent nuclear translocation of the pathogenic AR protein accounts for the gender-related pathogenesis, leading to the development of a potential hormonal therapy for this disorder (Katsuno et al., 2002). In this issue of *Neuron*, Sopher et al. (2004) report a new transgenic mouse model carrying human AR yeast artificial chromosome (YAC) with a prolonged CAG repeat. Their study reconfirmed the importance of nuclear accumulation of aberrant AR and ligand-dependent pathophysiology in SBMA. Since the expression of the transgene is controlled by its own promoter, the mRNA level of the mutant AR in this model is less than that in previous mouse models using potent exogenous promoters. This would account for the pathological distribution reminiscent of SBMA and the slow progression of motor disability. Among the conspicuous achievements in this study is the finding that the transgenic mice recapitulate the loss of lower motor neurons in SBMA. Whereas histopathological studies of autopsy cases with polyglutamine diseases show a tangible loss of neurons in lesions, a majority of transgenic mouse models demonstrate neuromuscular disability without detectable cell death (Zoghbi and Orr, 2000). This could be explained by the short life span and excessive expression of the causative polyglutamine protein in these mouse models. Symptomatic phenotypes with normal cell populations may indicate that the pathophysiology of polyglutamine disease rises from the dysfunction of neurons. This hypothesis in turn indicates the reversibility of the pathogenesis at the early stage of the diseases. In support of this view, the interruption of mutant gene

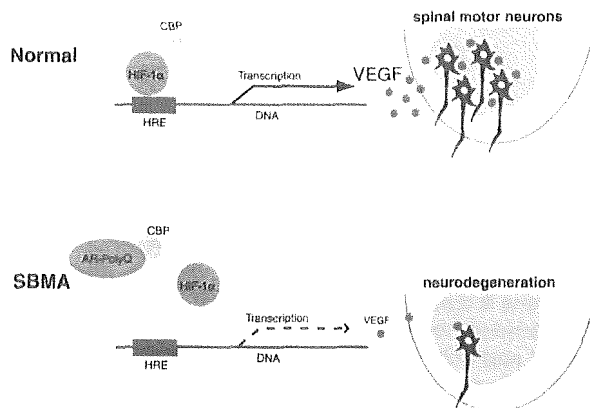


Figure 1. Possible Mechanism of VEGF-Related Motor Neuron Degeneration in SBMA

Hypoxia-inducible factor 1 α (HIF-1 α) binds to hypoxia-response element (HRE) in the promoter of vascular endothelial growth factor (VEGF), upregulating its transcription. This transactivating activity of HIF-1 α is facilitated through interaction with cAMP response element binding protein binding protein (CBP). In spinal and bulbar muscular atrophy (SBMA), the pathogenic androgen receptor (AR) containing expanded polyglutamine (polyQ) interacts with CBP, resulting in decreased level of VEGF. These processes appear to contribute to motor neuron degeneration in SBMA.

expression reversed the symptoms and histopathological features in a conditional mouse model of HD using a tet-regulation system (Yamamoto et al., 2000). Although this observation justifies medical intervention to mildly affected or presymptomatic patients, elucidating the precise mechanism giving rise to neuronal cell death is also essential for the development of therapies for polyglutamine diseases. The study of Sopher et al. appears to offer a striking insight into the pathophysiology of polyglutamine-induced motor neuron death, in their revelation that the interaction between pathogenic AR and CBP results in a reduced expression of vascular endothelial growth factor (VEGF), which appears to contribute to the neurodegeneration in SBMA.

VEGF, first discovered as a factor enhancing vascular permeability, plays a crucial role in physiological and pathological angiogenesis. Diverse biological effects of VEGF are facilitated by its receptor, VEGF-2, also termed kinase insert domain receptor (KDR). The gene expression of VEGF is drastically upregulated upon hypoxia in order to form new blood vessels. Hypoxia-inducible factors, HIF-1 α and HIF-2 α , mediate this cellular protective response through binding to hypoxia-response element (HRE) in the promoter of VEGF. The transactivating activity of HIF-1 α is facilitated through interaction with transcriptional coactivators such as CBP (Figure 1). The depletion of a single allele of VEGF results in embryonic lethality, whereas lack of the HRE sequence in the VEGF promoter leads to slowly progressive motor neuron degeneration (Oosthuysen et al., 2001). Knockin mice harboring a VEGF gene in which HRE is deleted demonstrate a late-onset motor neuron disease resembling SBMA and amyotrophic lateral sclerosis (ALS), suggesting a pivotal role for VEGF in neurodegeneration. The low expression level of VEGF in these mice results in loss of spinal motor neurons, axonal degeneration in

the peripheral nerve, and neurogenic muscular atrophy, all of which are pathological features of human motor neuron diseases. Moreover, the targeted disruption of HRE results in the marked exacerbation of motor neuron degeneration in transgenic mice carrying mutant superoxide dismutase 1 (SOD 1), the most frequent cause of familial ALS (Lambrechts et al., 2003). The deleterious effects of HRE deletion on motor neurons could be due to the suppression of favorable effects of VEGF: enhancement of blood supply and direct neuroprotection. Given that intraperitoneal administration of VEGF ameliorates ischemia-induced degeneration of spinal motor neurons in the aberrant VEGF knockin mice (Lambrechts et al., 2003), blood circulation insufficiency may cause neuromuscular phenotypes. Since VEGF protects cultured normal motor neurons from apoptotic stimuli, loss of these neurotrophic effects could also contribute to the pathogenesis of motor neuron degeneration due to HRE deletion.

The study of Sopher et al. shows that the reduction in the expression level of VEGF precedes the onset of neurogenic muscular atrophy, suggesting that the transcriptional alteration is a trigger, rather than a consequence, of neurodegeneration. The implication of VEGF in SBMA is also backed by the observation that an exogenous VEGF administration alleviates cytotoxicity induced by pathogenic AR with expanded polyglutamine in their cell model. In addition, CBP cotransfection augments VEGF level in the same cultured motor neurons, implying that the transactivating ability of CBP is suppressed by an aberrant protein-protein interaction with AR. This work sheds light on VEGF as a key player in the pathogenesis of polyglutamine-induced motor neuron degeneration, providing another therapeutic target for SBMA. The retrograde delivery of neurotrophic factors ameliorates neurodegeneration in mouse models of motor neuron diseases to some extent (Kaspar et al., 2003). It should be of value to investigate whether VEGF administration improves the polyglutamine-dependent pathogenesis in the SBMA mouse model of Sopher et al. Alternatively, the repressed transcription of VEGF in SBMA mice suggests that chronic hypoxia aggravates motor neuron degeneration, although its clinical implications have yet to be elucidated. Chronic ischemia, aggravated by lowered level of VEGF, appears to induce oxidative stress, which has been suggested to exacerbate neurodegenerative processes. It thus seems possible that polyglutamine-induced pathophysiology could be ameliorated by antioxidative therapy, which should be tested elsewhere.

A great deal of effort has been made to clarify the exact mechanism causing neuronal dysfunction and the process leading to cell death in polyglutamine diseases. Multiple pathophysiological steps may plunge neurons from dysfunction to death in the presence of an expanded polyglutamine tract. The transcriptional dysregulation of VEGF is likely to play an important role in polyglutamine-induced motor neuron death, since the HRE-deleted mice also showed loss of spinal motor neurons (Oosthuysen et al., 2001). However, whether this hypothesis accounts for the whole pathogenesis of SBMA remains to be resolved. Given that multiple mechanisms are involved in neurodegeneration, we need to clarify which genes, regulated by CBP or other factors,

are responsible for the pathogenesis of polyglutamine diseases. Such clarification would expand therapeutic options for these devastating disorders.

Masahisa Katsuno and Gen Sobue
Department of Neurology
Nagoya University Graduate School of Medicine
Nagoya 466-8550
Japan

Selected Reading

- Katsuno, M., Adachi, H., Kume, A., Li, M., Nakagomi, Y., Niwa, H., Sang, C., Kobayashi, Y., Doyu, M., and Sobue, G. (2002). *Neuron* 35, 843–854.
- Kaspar, B.K., Liado, J., Sherkat, N., Rothstein, J.D., and Gage, F.H. (2003). *Science* 301, 839–842.
- Lambrechts, D., Storkebaum, E., Morimoto, M., Del-Favero, J., Desmet, F., Marklund, S.L., Wyns, S., Thijs, V., Andersson, J., van Marion, I., et al. (2003). *Nat. Genet.* 34, 383–394.
- La Spada, A.R., Wilson, E.M., Lubahn, D.B., Harding, A.E., and Fischbeck, K.H. (1991). *Nature* 352, 77–79.
- McCampbell, A., Taye, A.A., Whitty, L., Penney, E., Steffan, J.S., and Fischbeck, K.H. (2001). *Proc. Natl. Acad. Sci. USA* 98, 15179–15184.
- Nucifora, F.C., Jr., Sasaki, M., Peters, M.F., Huang, H., Cooper, J.K., Yamada, M., Takahashi, H., Tsuji, S., Troncoso, J., Dawson, V.L., et al. (2001). *Science* 291, 2423–2428.
- Oosthuysen, B., Moons, L., Storkebaum, E., Beck, H., Nuyens, D., Brusselmans, K., Van Dorpe, J., Hellings, P., Gorselink, M., Heymans, S., et al. (2001). *Nat. Genet.* 28, 131–138.
- Sopher, B.L., Thomas, P.S., Jr., LaFevre-Bernt, M.A., Holm, I.E., Wilke, S.A., Ware, C.B., Jin, L.-W., Libby, R.T., Ellerby, L.M., and La Spada, A.R. (2004). *Neuron* 41, this issue, 687–699.
- Steffan, J.S., Bodai, L., Pallos, J., Poelman, M., McCampbell, A., Apostol, B.L., Kazantsev, A., Schmidt, E., Zhu, Y.Z., Greenwald, M., et al. (2001). *Nature* 413, 739–743.
- Sugars, K.L., and Rubinsztein, D.C. (2003). *Trends Genet.* 19, 233–238.
- Yamamoto, A., Lucas, J.J., and Hen, R. (2000). *Cell* 101, 57–66.
- Zoghbi, H.Y., and Orr, H.T. (2000). *Annu. Rev. Neurosci.* 23, 217–247.

Field strengths and sequences influence putaminal MRI findings in multiple system atrophy

H. Watanabe, MD; H. Fukatsu, MD; N. Hishikawa, MD; Y. Hashizume, MD; and G. Sobue, MD

Multiple system atrophy (MSA) is a sporadic neurodegenerative disease that is difficult to diagnose. MRI can show signal abnormalities such as putaminal hyperintensity, hyperintense putaminal rim, and significant putaminal hypointensity, strengthening a diagnosis of MSA.¹⁻⁷ However, these abnormalities are highly variable among the published cases and reports.¹⁻⁷ Differences of magnetic field strengths and sequences and pathologic features could explain such variability of putaminal signal changes, but the precise nature of putaminal signal changes remains unclear.¹⁻⁷

We report an MRI study of the cadaveric tissue from a patient with MSA performed to investigate putaminal signal changes with different magnetic field strengths and then correlated the findings with histopathologic observations.

Case report. A 54-year-old man first noticed gait disturbance at age 48 years and dysuria and erectile dysfunction at age 49 years, all of which steadily worsened. Neurologic examinations at age 50 years revealed urinary dysfunction and parkinsonism poorly responsive to L-dopa, including bradykinesia, rigidity, and postural instability. His condition worsened progressively, and he died of pneumonia 6 years after onset of illness.

Autopsy was performed 3 hours post-mortem. The brain was fixed in 10% buffered formalin. A 2-cm coronal section that included the putamen was used for MRI examination with 0.35-T (OPART, Japan) and 1.5-T (VISART, Japan) scanners using a surface coil. Images were obtained in the coronal plane using T2-weighted fast spin-echo (FSE) at 0.35 T and 1.5 T (2,000/120/5) and T2*-weighted gradient echo (GE) sequences (38/24/5; flip angle, 15) at 1.5 T. For all sequences, a 3-mm slice thickness, a field of view of 75 × 75 mm, and a matrix of 192 × 192 mm were used.

T2-weighted FSE at 0.35 T showed marked putaminal hyperintensity, whereas T2-weighted FSE at 1.5 T showed little signal change in the putamen except for mild hyperintensity in the outer margin. T2*-weighted GE at 1.5 T, representing the most sensitive MRI sequences for evaluation of putaminal iron deposition, showed low intensity (figure, A through C). For histopathologic evaluation, 5- μ m-thick paraffin-embedded sections were prepared from the same position and stained with hematoxylin and eosin, Holzer, Gallyas-Braak, Bodian, and Prussian blue stains. Neuronal loss and gliosis were noted, as were glial cytoplasmic inclusions, all typical histopathologic findings for MSA. The Holzer stain showed severe gliosis predominantly in the dorsolateral putamen (figure, D). No calcification was present. Extracellular and intracellular iron deposits were present extensively in this area (figure, E). The high signal intensity on T2-weighted FSE at 0.35 T was highly consistent with the distribution of gliosis. Conversely, the low intensity on T2*-weighted GE at 1.5 T corresponded well to the region of iron deposits.

Discussion. This is the first study to correlate putaminal MRI findings at different magnetic field strengths and sequences in postmortem MSA brain with histologic findings. Although artifact from formalin and varying relaxation rates caused by a different hydration state of the tissue should be considered, direct comparison of post-mortem MRI and histologic findings would be beneficial particularly for understanding MR signal differences in the putamen of patients with MSA because putaminal findings at autopsy could differ from those at examination of MRI during life.

MRI using FSE at 1.5 T, which is used widely for diagnosis of MSA, showed only mild hyperintensity in the outer putaminal margin, which can be observed even in healthy subjects. Conversely, FSE at 0.35 T and GE at 1.5 T revealed significant putaminal hyperintensity and hypointensity. Histopathologic study showed severe gliosis and an increase in ferritin deposition, particularly in the dorsolateral putamen. Gliosis probably increased signal intensity in T2-weighted images, whereas ferritin enhanced T2 relaxation in the order FSE at 0.35 T, FSE at 1.5 T, and GE at 1.5 T. Taken together, topography of gliosis predominantly in dorsolateral parts, severities of gliosis and iron deposits, and magnetic field strengths and sequences would determine the putaminal MRI findings and can result in a normal putaminal appearance under FSE at 1.5 T despite the presence of pathologic

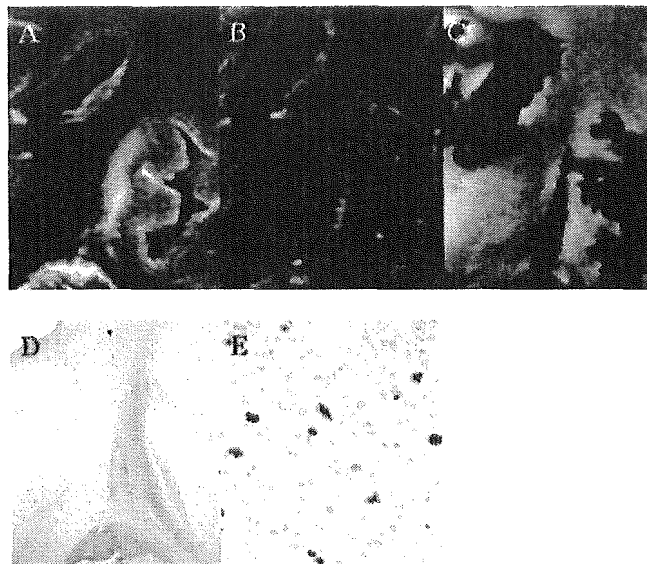


Figure. (A) MRI operated at T2-weighted fast spin-echo (FSE) at 0.35 T. Significant putaminal hyperintensity is evident. (B) MRI operated at T2-weighted FSE at 1.5 T. The greater part of the putamen shows iso-intensity except for mild hyperintensity of the rim at the outer margin. (C) MRI operated at T2*-weighted gradient echo at 1.5 T. Severe putaminal hypointensity is observed. (D) Holzer stain. Exclusive severe gliosis is seen in the putamen. (E) Prussian blue stain. An increase in ferritin deposits is widespread in the putamen. Original magnification, ×400.

change. In contrast, the higher insensitivity to paramagnetic effects can provide the hyperintensity at 0.35 T.

Putaminal hyperintensity in MRI was first described as a finding typical to MSA.¹ Many subsequent reports have confirmed this, but sensitivity and specificity were found to be highly variable.²⁻⁷ In MR survey of patients with MSA, it should be considered that histopathologic features differentially affect MR findings at different magnetic field strengths and sequences.

From the Departments of Neurology (Drs. Watanabe, Hishikawa, and Sobue) and Radiology (Dr. Fukatsu), Nagoya University Graduate School of Medicine, Japan; and Institute for Medical Science of Aging (Dr. Hashizume), Aichi Medical University, Japan.

Received May 30, 2003. Accepted in final form October 17, 2003.

Address correspondence and reprint requests to Dr. Gen Sobue, Department of Neurology, Nagoya University Graduate School of Medicine, Nagoya 466-8550 Japan; e-mail: sobueg@med.nagoya-u.ac.jp

Copyright © 2004 by AAN Enterprises, Inc.

References

1. Savoirdo M, Strada L, Girotti F, et al. MR imaging in progressive supranuclear palsy and Shy-Drager syndrome. *J Comput Assist Tomogr* 1989;13:555-560.
2. Schwarz J, Weis S, Kraft E, et al. Signal changes on MRI and increases in reactive microgliosis, astrogliosis, and iron in the putamen of two patients with multiple system atrophy. *J Neurol Neurosurg Psychiatry* 1996;60:98-101.
3. Schrag A, Kingsley D, Phatouros C, et al. Clinical usefulness of magnetic resonance imaging in multiple system atrophy. *J Neurol Neurosurg Psychiatry* 1998;65:65-71.
4. Kraft E, Schwarz J, Trenkwalder C, Vogl T, Pfluger T, Oertel WH. The combination of hypointense and hyperintense signal changes on T2-weighted magnetic resonance imaging sequences: a specific marker of multiple system atrophy? *Arch Neurol* 1999;56:225-228.
5. Watanabe H, Saito Y, Terao S, et al. Progression and prognosis in multiple system atrophy: an analysis of 230 Japanese patients. *Brain* 2002;125:1070-1083.
6. Kraft E, Trenkwalder C, Auer DP. T2*-weighted MRI differentiates multiple system atrophy from Parkinson's disease. *Neurology* 2002;59:1265-1267.
7. Bhattacharya K, Saadia D, Eisenkraft B, et al. Brain magnetic resonance imaging in multiple-system atrophy and Parkinson's disease: a diagnostic algorithm. *Arch Neurol* 2002;59:835-842.

Sweet relief for Huntington disease

Masahisa Katsuno, Hiroaki Adachi & Gen Sobue

Oral delivery of a simple, nontoxic sugar molecule alleviates symptoms of Huntington disease in a mouse model (pages 148–154).

A CAG repeat was first pinned to a neurological disorder—spinal and bulbar muscular atrophy (SBMA)—in 1991 (ref. 1). The pathological influence of the affected gene, an androgen receptor, eventually paled beside the growing realization that the repeat itself was key to the disease. A number of other neurological diseases have since been linked to glutamine-encoding CAG repeats, most prominent among them Huntington disease.

Despite the excitement they have sparked, these discoveries have as yet done little to improve the lives of patients, including more than 35,000 with Huntington disease in the United States. In this issue, Tanaka *et al.* move us closer to reaping the benefits of this decade of research. The authors report that in mouse models of Huntington disease, treatment with a nontoxic sugar substance can prevent the development of the brain pathology associated with Huntington disease, and can delay the progress of symptoms such as motor dysfunction. The approach stands out as the most exciting therapeutic prospect to date for Huntington disease, and also holds promise for the entire class of polyglutamine disorders.

In addition to Huntington disease and SBMA, other polyglutamine disorders include several forms of spinocerebellar ataxia, as well as dentatorubral pallidolysian atrophy². Outside of the polyglutamine stretch, each causative protein seems unrelated, and removal of the causative protein genetically or by other means does not result in disease in humans or animal models². Yet the diseases show phenotypic similarities. The clinical features depend at least partially on the number of CAG repeats, and are influenced by the meiotic instability of the repeat length. These clinical and genetic similarities imply that polyglutamines induce toxicity, although loss of the normal function of causative proteins may influence the disease³.

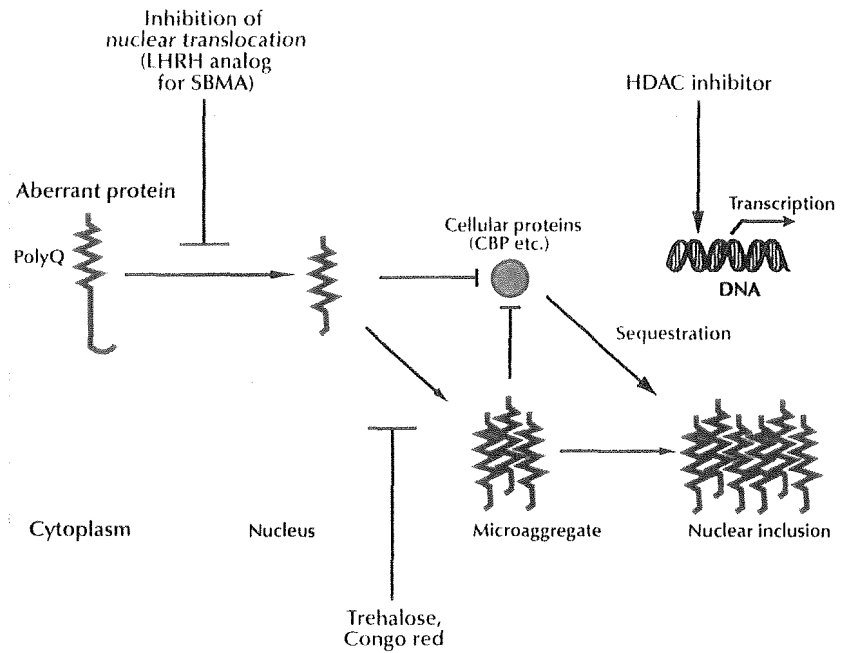


Figure 1 Therapeutic approaches for polyglutamine diseases. Several approaches attempt to mitigate the toxicity of polyglutamine (poly Q) tract-containing proteins. Leuprorelin prevents nuclear uptake of mutant androgen receptor, resulting in the rescue of neuromuscular phenotypes of SBMA. Histone deacetylase inhibitors ameliorate transcription of affected cells. Tanaka *et al.* found that a disaccharide, trehalose, inhibits aggregation of a protein with an expanded polyglutamine tract, especially in the nucleus (as does Congo red). LHRH, luteinizing hormone-releasing hormone; CBP, CREB-binding protein.

How do the glutamine repeats affect the cell? The expansion of the polyglutamine tract alters protein conformation, resulting in the formation of insoluble aggregates. These aggregates sequester normal cellular proteins such as transcription factors, heat shock proteins, ubiquitin, and proteasome components. The propensity of the polyglutamine-containing proteins to aggregate depends on the length of the polyglutamine stretch and is enhanced by protein cleavage through caspase activation.

Patients with polyglutamine diseases show loss of specific types of neurons. The cells that do not die contain inclusions rich in polyglutamine-containing proteins, mainly in the nucleus. These inclusions are found in the vulnerable neurons, implying a direct role in pathogenesis. Whether these aggregates are toxic—a notion supported by a

large body of evidence—or reflect a protective response is controversial.

A dramatic study earlier this year bolstered arguments in favor of toxicity. Injection of the dye Congo red prevented formation of nuclear inclusions and alleviated symptoms in a mouse model of Huntington disease⁴.

Tanaka *et al.*, favoring the notion that the aggregates are toxic, sought a new aggregation inhibitory therapy for Huntington disease⁵. The authors first used an *in vitro* aggregate formation assay, with myoglobin containing an expanded polyglutamine tract as a target molecule. Using this screening system, they discovered that disaccharides potently inhibited aggregate formation. Trehalose, the most effective disaccharide, selectively stabilized a protein containing a long polyglutamine tract, but not a protein with the normal number of glutamines. The authors confirmed this stabi-

Masahisa Katsuno, Hiroaki Adachi and Gen Sobue are in the Department of Neurology, Nagoya University Graduate School of Medicine, Nagoya, 65 Tsurumai-cho, Showa-ku, Nagoya 466-8550, Japan.
e-mail: sobueg@med.nagoya-u.ac.jp

lization in a cell model expressing the aberrant form of huntingtin, the causative protein of Huntington disease. The stabilization of myoglobin with an elongated polyglutamine tract results⁶ accounts for the trehalose-mediated suppression of aggregate formation.

The authors went on to test transgenic mouse models of Huntington disease. They found that trehalose-treated mice had fewer nuclear inclusions than untreated mice. Trehalose also improved motor dysfunction and prolonged survival, without any deleterious side effects. The extremely low toxicity and high water-solubility of this compound make this an attractive therapeutic approach, although the therapeutic effects seem to result from prevention of new aggregate formation, not from reversal of the pathology. The data reinforce the rationale of aggregation-inhibitory therapy for polyglutamine diseases (Fig. 1). Trehalose is now ready for phase 1 safety trials in humans.

Other approaches to polyglutamine disease also show promise. Nuclear accumulation of polyglutamine-containing proteins before aggregate formation is probably an essential step in pathogenesis. A mutation that inactivates the nuclear localization signal in ataxin-1, the causative protein in spinocerebellar ataxia-

1, nullifies polyglutamine-induced neurodegeneration in a transgenic mouse model⁷. In cell culture, chemically synthesized polyglutamine peptides induce neuronal cell death only when they are directed into the nucleus⁸. These observations suggest that nuclear-directed transport of mutant proteins is an alternative target of intervention (Fig. 1), although cytosolic events should not be neglected³.

Androgen deprivation therapy in a transgenic mouse model of SBMA clearly demonstrates the usefulness of this therapeutic strategy⁹. A luteinizing hormone-releasing hormone analog, leuprorelin, prevents nuclear translocation of polyglutamine-containing androgen receptor protein, resulting in a significant improvement of disease⁹. A clinical trial with leuprorelin, currently under way in Japan, should clarify the clinical benefit of this drug for SBMA patients.

Transcriptional dysregulation, an event downstream of polyglutamine aggregation, can also be targeted (Fig. 1). Transcriptional coactivators including CREB-binding protein are sequestered in the inclusion, and are also enfeebled by interaction with soluble polyglutamine tract-containing proteins³. An increase in acetylation of nuclear histone proteins, facilitated by histone deacetylase

inhibitors, ameliorates neurodegeneration in a mouse model of Huntington disease^{10,11}. These compounds have also been used for patients with malignancies. Clinical trials of histone deacetylase inhibitors should be planned carefully, however, taking the hazardous side effects into account.

The promising results of these preclinical studies are ushering in a new era in polyglutamine research: the therapeutic stage. The new investigations also encourage us to continue to search for new, clinically applicable compounds such as aggregation inhibitors. The intensive basic research is bearing fruit, and shows promise of continuing to do so as we move into clinical trials.

1. La Spada, A.R. *et al. Nature* **352**, 77–79 (1991).
2. Zoghbi, H.Y. & Orr, H.T. *Annu. Rev. Neurosci.* **23**, 217–247 (2000).
3. Ross, C.A. *Neuron* **35**, 819–822 (2002).
4. Sanchez, I. *et al. Nature* **421**, 373–379 (2003).
5. Tanaka, M. *et al. Nat. Med.* **10**, 148–154 (2004).
6. Tanaka, M. *et al. J. Biol. Chem.* **276**, 45470–45475 (2001).
7. Klement, I.A. *et al. Cell* **95**, 41–53 (1998).
8. Yang, W. *et al. Hum. Mol. Genet.* **11**, 2905–2911 (2003).
9. Katsuno, M. *et al. Nat. Med.* **9**, 768–773 (2003).
10. Hockly, E. *et al. Proc. Natl. Acad. Sci. USA* **100**, 2041–2046 (2003).
11. Ferrante, R.J. *et al. J. Neurosci.* **23**, 9418–9427 (2003).

PAPER

Multiple regional ^1H -MR spectroscopy in multiple system atrophy: NAA/Cr reduction in pontine base as a valuable diagnostic marker

H Watanabe, H Fukatsu, M Katsuno, M Sugiura, K Hamada, Y Okada, M Hirayama, T Ishigaki, G Sobue

J Neurol Neurosurg Psychiatry 2004;75:103-109

See end of article for authors' affiliations

Correspondence to:
Gen Sobue, MD,
Department of Neurology,
Nagoya University
Graduate School of
Medicine, Nagoya 466-
8550 Japan; sobueg@
med.nagoya-u.ac.jp

Received
20 December 2002
In revised form
31 March 2003
Accepted 17 May 2003

Objective: We performed ^1H -MR spectroscopy (^1H -MRS) on multiple brain regions to determine the metabolite pattern and diagnostic utility of ^1H -MRS in multiple system atrophy (MSA).

Methods: Examining single voxels at 3.0 T, we studied metabolic findings of the putamen, pontine base, and cerebral white matter in 24 MSA patients (predominant cerebellar ataxia (MSA-C), $n=13$), parkinsonism (MSA-P), $n=11$), in 11 age and duration matched Parkinson's disease patients (PD) and in 18 age matched control subjects.

Results: The *N*-acetylaspartate to creatine ratio (NAA/Cr) in MSA patients showed a significant reduction in the pontine base ($p<0.0001$) and putamen ($p=0.02$) compared with controls. NAA/Cr in cerebral white matter also tended to decline in long standing cases. NAA/Cr reduction in the pontine base was prominent in both MSA-P ($p<0.0001$) and MSA-C ($p<0.0001$), and putaminal NAA/Cr reduction was significant in MSA-P ($p=0.009$). It was also significant in patients who were in an early phase of their disease, and in those who showed no ataxic symptoms or parkinsonism, or did not show any MRI abnormality of the "hot cross bun" sign or hyperintense putaminal rims. NAA/Cr in MSA-P patients was significantly reduced in the pontine base ($p=0.001$) and putamen ($p=0.002$) compared with PD patients. The combined ^1H -MRS in the putamen and pontine base served to distinguish patients with MSA-P from PD more clearly.

Conclusions: ^1H -MRS showed widespread neuronal and axonal involvement in MSA. The NAA/Cr reduction in the pontine base proved highly informative in the early diagnosis of MSA prior to MRI changes and even before any clinical manifestation of symptoms.

Multiple system atrophy (MSA) is a sporadically occurring neurodegenerative disease that presents parkinsonism, cerebellar ataxia, autonomic failure, and pyramidal signs of varying severity during the course of illness.¹⁻³ Neuropathological findings consist of a varying neuronal loss, gliosis, and demyelination with widespread regional involvement, particularly including the striatonigral, olivopontocerebellar, and autonomic nervous systems.⁴⁻⁶ The tempo and progression of multiple system involvement vary widely among individual MSA patients and have been closely related to both functional deterioration and prognosis by clinical evaluation.⁷ Thus, assessing the multi-regional involvement in MSA is essential for accurate diagnosis, counselling of patients and families, optimal management of symptoms, and the usefulness of future therapeutic trials.

Proton magnetic resonance spectroscopy (^1H -MRS) is a valuable non-invasive MR technique for monitoring brain metabolism *in vivo*.⁸⁻¹⁸ The major peaks of the ^1H -MRS spectrum, corresponding to *N*-acetylaspartate (NAA), creatine (Cr), and choline (Cho) containing phospholipids, have been used to evaluate neuronal loss and active myelin breakdown. The ratio of NAA to Cr (NAA/Cr) is considered a metabolic marker reflecting the functional status of neurones and axons in the brain, with a decrease indicating neuronal or axonal loss or dysfunction. Previous studies using ^1H -MRS in MSA with predominant parkinsonism (MSA-P) reported a significant NAA/Cr reduction in the striatum compared with Parkinson's disease (PD) patients and normal subjects.¹¹⁻¹⁴ However, the pontine base and cerebral white matter, which are also pathologically involved

in MSA, have not been fully assessed by ^1H -MRS. Recent technical innovations have permitted ^1H -MRS at higher magnetic field strengths.¹⁹⁻²¹ Multi-regional data can be obtained from single voxel ^1H -MRS within a short examination time with increasing signal to noise ratio (SNR).

Our purpose was to assess the extent of multiple system involvement in patients with MSA by using multiple regional single voxel ^1H -MRS including the putamen, pontine base, and cerebral white matter (CWM), and to further assess the diagnostic value of the regional ^1H -MRS.

METHODS

All patients and control subjects gave written informed consent. The MR protocol was approved by the Ethics Committee of the Nagoya University School of Medicine. Twenty four patients with MSA (12M, 12F; mean (SD) age 61 (7) years old), 11 patients with PD (5M, 6F; 63 (9) years old), and 18 control subjects with no history of any neurological disease (10M, 8F; 59 (7) years old) were studied. No significant differences in male to female ratio or age were noted among the three groups. The duration from initial

Abbreviations: Cho, choline; Cr, creatine; CWM, cerebral white matter; HCB, "hot cross bun"; HPR, hyperintense rim; MRI, magnetic resonance imaging; MRS, magnetic resonance spectroscopy; MSA, multiple system atrophy; MSA-C, multiple system atrophy with cerebellar ataxia predominant; MSA-P, multiple system atrophy with parkinsonism predominant; NAA, *N*-acetylaspartate; PD, Parkinson's disease; SNR, signal to noise ratio; VOI, volume of interest.

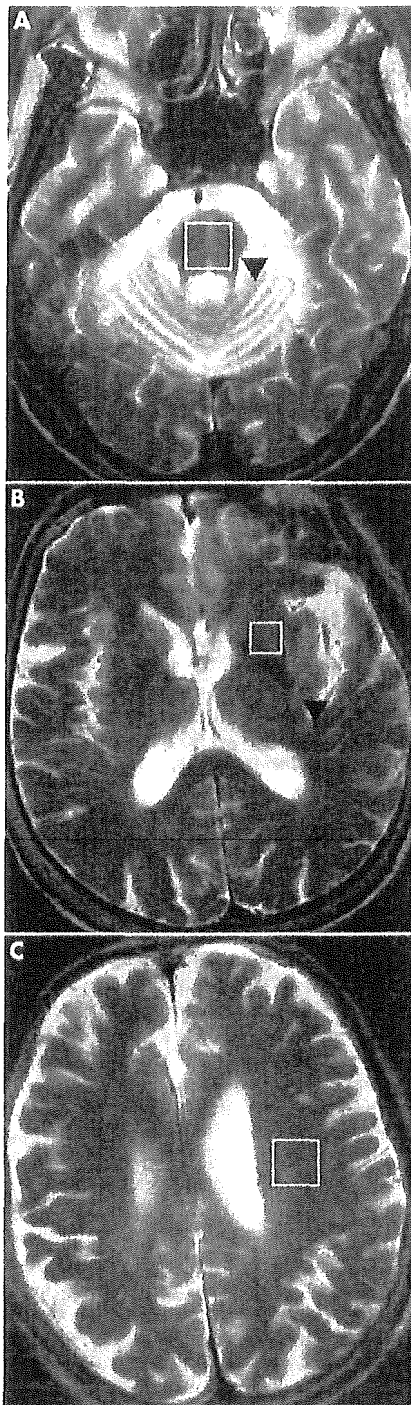


Figure 1 Location of volumes of interest are shown by squares in the pontine base (A), putamen (B), and white matter of the frontal lobe (C). Additionally, in these images, an HCB sign is present in the pons (A), as is a hyperintense putaminal rim (B). Axial T2 weighted images (3.0 T; TR: 3970, TE: 80), with respective findings are indicated by arrowheads.

symptoms to MRI and MRS evaluation also showed no differences between MSA and PD patients (MSA; 3.7 (2.4) years; PD; 4.4 (2.2) years, $p > 0.4$). Diagnoses of all MSA and PD patients were "probable" according to established diagnostic criteria.^{3,22} As for subtypes of MSA,

cerebellar dysfunction (MSA-C) predominated in 13 patients and parkinsonism (MSA-P) in 11. We classified patients into two groups according to the presence of parkinsonian signs in MSA, based on the consensus statement for MSA diagnosis. Patients with bradykinesia plus at least one sign of either rigidity, postural instability, or tremor were considered to manifest parkinsonism and designated as "parkinsonism+", while others were taken to be "parkinsonism-". As for cerebellar dysfunction, patients with gait ataxia plus at least one sign of ataxic dysarthria, limb ataxia, or sustained gaze evoked nystagmus were considered "ataxia+", and others as "ataxia-" based on the consensus criteria.³ Six of nine MSA-P patients and all PD patients were taking medication for parkinsonism (benserazide/levodopa 25/100 mg, or carbidopa/levodopa 10/100 mg, two or three times daily). All PD patients showed a good response to treatment.

MRI and ¹H-MRS were performed with a 3.0 T system (Bruker, Ettlingen, Germany) using a standard head coil with circular polarisation. The imaging protocol consisted of sagittal T1 weighted spin echo sequences (repetition time (TR), 460 ms; echo time (TE), 14 ms) and transverse T2 weighted sequences (TR, 3970 ms; TE, 80 ms). Slice thickness was 6 mm with a 1.2 mm gap and a 512×384 matrix. We evaluated whether a "hot cross bun" (HCB) sign was present in the pons and whether the putamen showed a hyperintense rim (HPR), according to the criteria described in previous reports (fig 1A, B).^{7,23-26} The spectroscopic volume of interest (VOI) was placed in the pontine base (2.2 to 3.4 cm³), the putamen (1 cm³), and the CWM (3.4 cm³; fig 1A to C). Voxel size was chosen to be as small as possible while maintaining an acceptable SNR in order to minimise the partial volume effect. Care was taken not to incorporate cerebrospinal fluid spaces within a VOI. The VOI in the putamen was placed on the more affected side, and the frontal lobe VOI was ipsilateral to the putaminal VOI. ¹H-MR spectra were acquired using a point resolved spectroscopy sequence with chemical shift selective water suppression. Spectral parameters were as follows: TR: 2000 ms; TE: 30 ms; averages: 256 in the putamen, and 64 each in the centrum semiovale and pons; data points: 1024. A shimming procedure focused on the water signal was performed to obtain a uniform and homogenous magnetic field. After Fourier transformation and zero order phase correction, relative metabolite concentrations for NAA at 2.0 ppm, Cr at 3.0 ppm, and Cho at 3.2 ppm were determined by Lorentzian curve fitting of the corresponding resonance in the frequency spectra. The baseline was corrected for purposes of data presentation. From these data, the metabolite ratios NAA/Cr, and Cho/Cr were determined as semiquantitative values. Post-procedural processing was performed by the same radiologist (HF). All preconditioning, spectroscopic measurements, and processing were performed with Paravision 2.01 software (Bruker). Total examination time including MRI and ¹H-MRS was <1 hour. One MSA-C patient with severe pontine atrophy was excluded because a good pontine spectrum could not be obtained.

Values obtained were entered into a database for further statistical analysis. The Mann-Whitney U test and the Kruskal-Wallis test for nonparametric statistics were performed as appropriate. When the Kruskal-Wallis test indicated differences among groups, in a multiple comparison analysis, Scheffé's test was used to identify which group differences accounted for the significant p value. Relationships of NAA/Cr reduction to duration of illness were analysed using Pearson's correlation coefficient. Calculations were performed using the Stat View statistical software package (Abacus Concepts, Berkeley, CA, USA). Statistical significance was defined as $p < 0.05$.

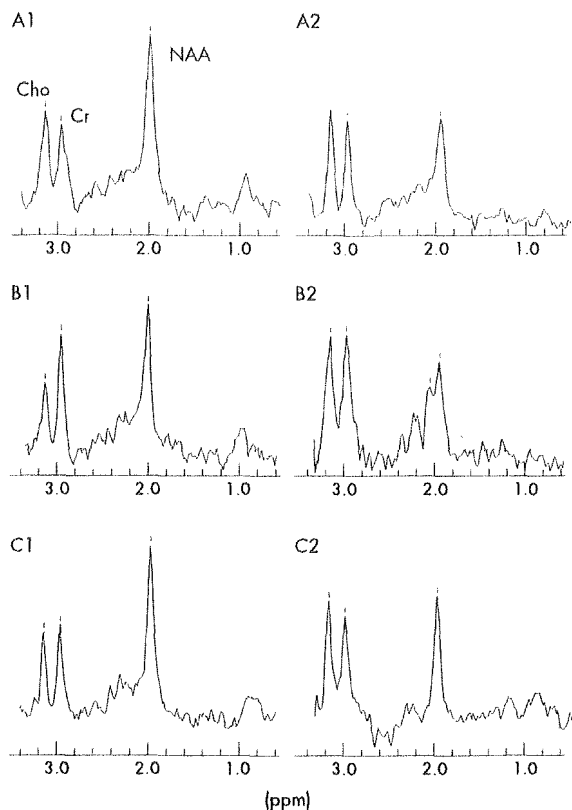


Figure 2 Representative ¹H-MRS spectra from control and MSA subjects. A1, B1, and C1 represent spectra from a control subject's pontine base, putamen, and cerebral white matter, respectively. A2, B2, and C2 represent spectra from those same three regions in an MSA patient. NAA, N-acetylaspartate; Cho, choline; Cr, creatine; MSA, multiple system atrophy; CWM, cerebral white matter.

RESULTS

Widespread NAA/Cr reduction in MSA in multiple regional ¹H-MRS

A representative MSA patient (fig 2) showed a marked reduction of the NAA peak in the pontine base, putamen, and cerebral white matter compared with controls. NAA/Cr was significantly reduced in the pontine base of MSA patients ($p < 0.0001$) and in the putamen ($p = 0.02$) compared with controls. MSA patients also showed a lower NAA/Cr in cerebral white matter than controls, but this difference was not statistically significant ($p = 0.12$). Cho/Cr was only slightly increased in MSA, and no significant differences were found among the three groups for the pontine base, putamen, and CWM.

Prominent NAA/Cr reduction in pontine base in both MSA-C and MSA-P

Significant reductions of NAA/Cr were evident in the pontine base, putamen, and CWM in MSA-C and MSA-P compared with controls (fig 3A–C). MSA-C patients showed a significant reduction of NAA/Cr in the pontine base ($p < 0.0001$) and CWM ($p = 0.02$), but not in the putamen. MSA-P patients showed a significant reduction of NAA/Cr in the pontine base ($p < 0.0001$) and putamen ($p = 0.009$) but not in the CWM. These observations indicate that the NAA/Cr reduction in the pontine base was significant in both MSA-C and MSA-P. Cho/Cr

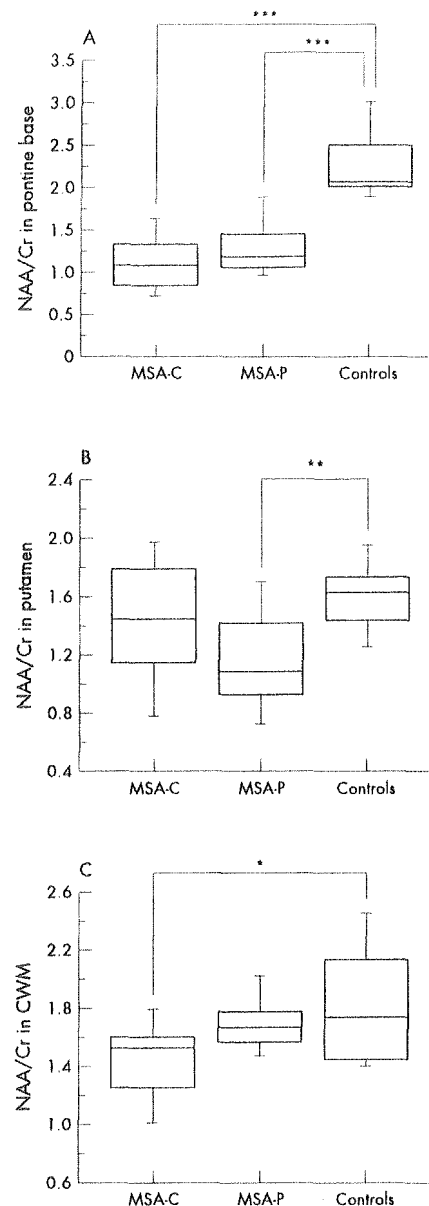


Figure 3 Box and whisker plot of the NAA/Cr ratio. Horizontal lines indicate median values. Boxes extend from the 25th to the 75th percentile. A, B, and C respectively show NAA/Cr in the pontine base, putamen, and cerebral white matter, comparing MSA-C, MSA-P, and control subjects. * $p = 0.02$, ** $p = 0.009$, and *** $p < 0.0001$ by Scheffé's test, respectively. NAA, N-acetylaspartate; Cr, creatine; Cho, choline containing component; MSA-C, multiple system atrophy with cerebellar ataxia predominant; MSA-P, multiple system atrophy with parkinsonism predominant.

was not changed in MSA-P or MSA-C compared with controls.

Relation of NAA/Cr reduction in pontine base with disease phase, motor symptoms and MRI abnormalities in MSA

In terms of disease duration, the NAA/Cr reduction was most significant in the pontine base of patients with MSA even in an early phase of illness (fig 4). A tendency toward an inverse

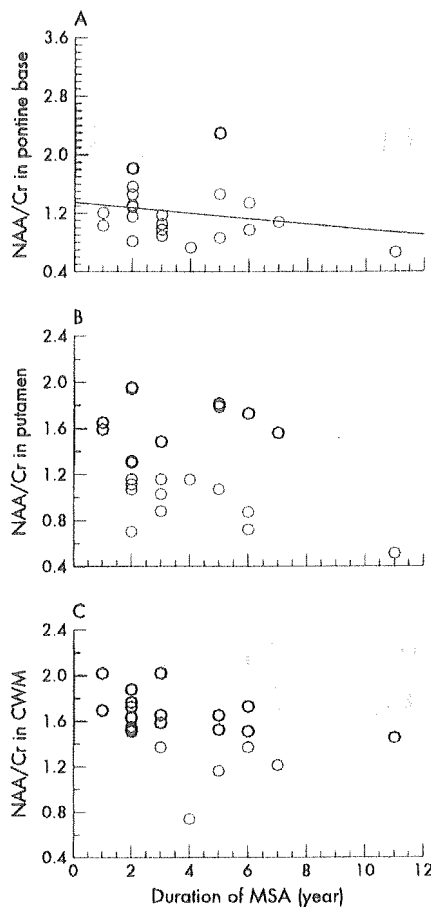


Figure 4 Correlation with duration of MSA of individual NAA/Cr ratios in the pontine base (A), putamen (B), and cerebral white matter (C). The shaded area corresponds to the mean (SD) of NAA/Cr in control subjects. NAA, N-acetylaspartate; Cr, creatine; CWM, cerebral white matter; MSA, multiple system atrophy.

relationship between disease duration and NAA/Cr in the three regions was observed, but did not attain significance (pontine base: $r = -0.24$, $p = 0.29$; putamen: $r = -0.32$, $p = 0.14$; CWM: $r = -0.41$, $p = 0.06$). NAA/Cr in the pontine base was significantly reduced compared with controls even in patients who did not show ataxic symptoms ($p = 0.0006$, fig 5A-1). However, NAA/Cr in the putamen and white matter was not reduced in patients with ataxia (fig 5B-1, C-1). NAA/Cr in the putamen was markedly decreased in MSA patients with parkinsonism ($p = 0.02$, Fig 5B-2), whereas patients without it exhibited no significant reduction compared with controls. NAA/Cr reduction in the pontine base, on the other hand, was significant ($p < 0.0001$) irrespective of parkinsonism (Fig 5A-2).

The MRI revealed the HCB sign in the pontine base in eleven MSA patients (46%) and the HPR sign in six (25%). A significant reduction of NAA/Cr was seen in the pontine base even in patients without ($p < 0.0001$) as well as in those with an HCB sign ($p < 0.0001$; fig 5A-3). In the putamen and cerebral white matter, NAA/Cr values did not show any significant difference irrespective of the HCB sign (fig 5B-3, C-3). Moreover, NAA/Cr significantly decreased in the pontine base in patients both with and without HPR (fig 5A-4). NAA/Cr in the putamen and cerebral white matter did not show any significant differences

irrespective of HPR signs (fig 5B-4, C-4). Cho/Cr had no significant relationship to ataxic, parkinsonism, or MRI abnormalities.

NAA/Cr in pontine base in MSA-P and PD

NAA/Cr reduction in the pontine base was highly significant in patients with MSA-P compared with both controls and PD ($p < 0.0001$, $p = 0.001$; fig 6A). NAA/Cr in the putamen in MSA-P patients also showed a significant decrease compared with both controls and PD ($p = 0.003$, $p = 0.002$; fig 6B). No significant differences in NAA/Cr were noted in cerebral white matter between MSA-P and PD. These data indicate that the NAA/Cr reduction in the pontine base is a valuable marker to discriminate MSA-P from PD. In addition, combining individual NAA/Cr values for the pontine base and putamen further reduced the overlap between MSA-P and PD (fig 6D), suggesting that a combined assessment of the pontine base and putamen was more effective in discriminating between MSA-P and PD than individual area assessments. Cho/Cr did not display any significant changes in the pontine base, putamen or cerebral white matter.

DISCUSSION

We demonstrated widespread NAA/Cr reduction in the pontine base, putamen and in some cases, in the cerebral hemisphere, but no significant Cho/Cr alteration in patients with MSA using localised ^1H -MRS at 3.0 T. In this study, absolute metabolite concentrations were not measured. However, the specific conditions that may change the total Cr signal, such as trauma, hyperosmolar conditions, hypoxia, stroke, and tumours, were not included. Age was matched among MSA, PD, and control groups. Moreover, quantitative studies did not show significant Cr changes between MSA patients and control subjects.¹¹⁻¹⁶ Thus, the reduction of the NAA/Cr ratio in the present study can be considered due to a selective decrease in NAA levels.

NAA has been immunohistochemically demonstrated to localise almost exclusively within neurones and axons,²⁷⁻²⁹ but some in vitro studies have also detected NAA expression in mature, immature, and undifferentiated oligodendrocytes.³⁰⁻³² Nevertheless, according to a recent study, in vivo MRS measurements of NAA remain axon specific, with no oligodendrocytes, nonproliferating oligodendrocyte progenitor cells, or myelin contributing to detectable NAA in the mature CNS.³¹ This result supports the view that the widespread NAA/Cr reductions observed in this study ultimately reflect widespread neuronal and axonal involvement in MSA, although oligodendrocytes might influence the NAA levels to some degree.

The striking observation in this study is that the NAA/Cr reduction in the pontine base was the most significant among the three regions examined. That reduction was detected in the early phase of illness even in patients with no symptoms of ataxia or parkinsonism, or in patients without MRI abnormality of the HCB sign. Moreover, the pontine NAA/Cr reduction was significant even in MSA-P patients. In addition, NAA/Cr reductions in the pontine base were seen even in patients with no HPR sign in the lateral putamen. These observations suggest that NAA/Cr reduction in the pontine base is an accurate diagnostic marker for MSA even in patients in an early stage and a pre-symptomatic phase of ataxia or parkinsonism. The diagnostic focus of ^1H -MRS in MSA has been on the putamen,¹¹⁻¹⁴ whereas our results unequivocally demonstrated that MRS abnormality can be detected sooner and more universally in the pontine base than in the putamen in the course of the disease. The question is why a significant NAA/Cr reduction can be detected more readily in the pontine base than in the putamen. One reason may be that neuroaxonal degeneration

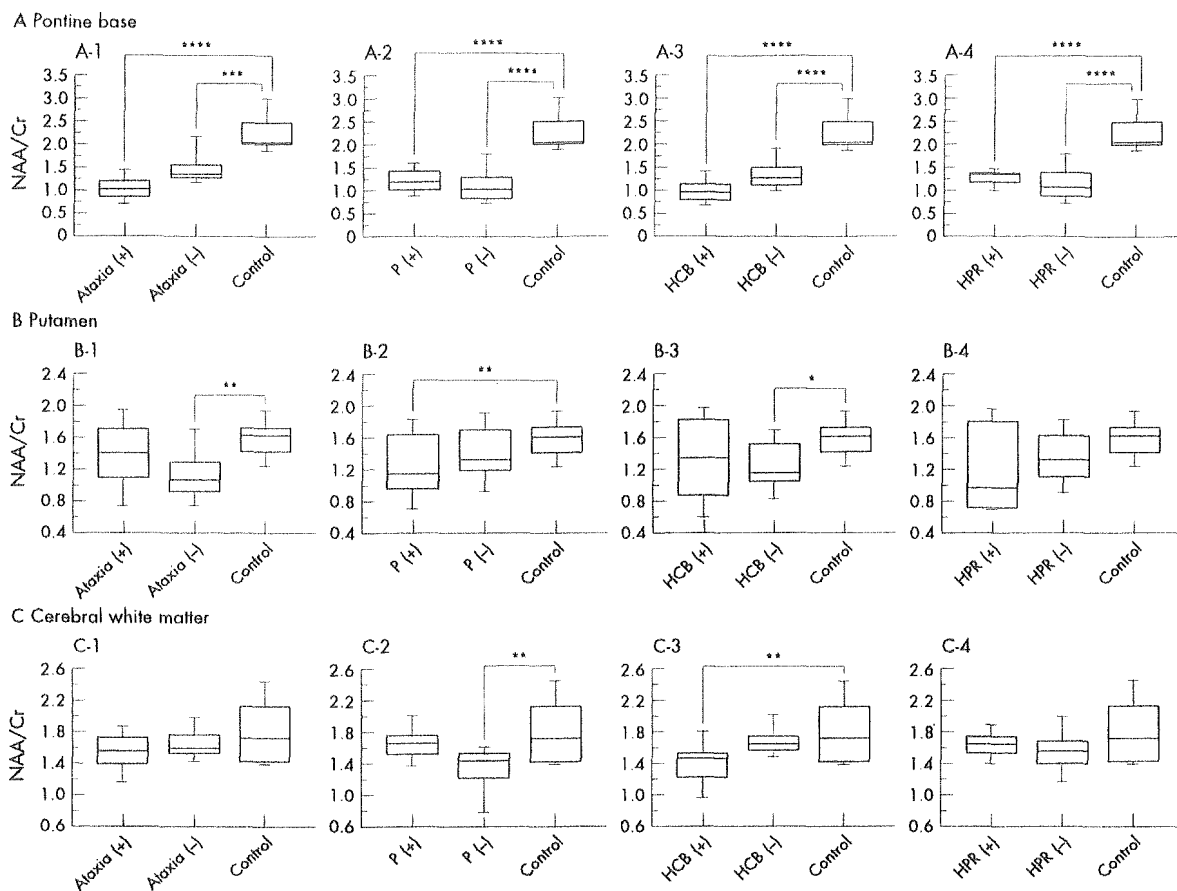


Figure 5 NAA/Cr in the pontine base (A), putamen (B), and cerebral white matter (C) for MSA patients classified in terms of clinical features of ataxia (+ or -; A-1, B-1, C-1), parkinsonism (P; + or -; A-2, B-2, C-2), HCB on MRI (+ or -; A-3, B-3, C-3), and hyperintense putaminal rim (HPR) on MRI (+ or -; A-4, B-4, C-4). +, Presence; -, absence. * $p=0.047$, ** $p=0.02$, *** $p=0.0006$, and **** $p<0.0001$ by Scheffé's test, respectively. NAA, N-acetylaspartate; Cr, creatine; MSA, multiple system atrophy; CWM, cerebral white matter.

in the pons would be more extensive than in the putamen. As the pontine base consists of the axons and neurones specifically involved in MSA (for example fibres of cerebellar inflow and outflow, corticospinal tracts and transverse pontine tracts), subclinical involvement of such fibres could be detected as a reduction of NAA/Cr. Furthermore, because, as we demonstrated previously, MSA-C is significantly more prevalent in Japan than MSA-P, compared with white populations in the western countries,⁷ the cerebellar pontine system should be more profoundly involved in Japanese MSA patients. A second possibility is that the volume effect due to putaminal atrophy would ultimately include the neighbouring normal tissues in the VOI of the MRS, influencing the degree of the NAA/Cr reduction. As atrophy of the putamen is severe in certain patients, the size of the VOI is a limiting factor in ¹H-MRS for maintaining an acceptable SNR. Such volume effects due to putaminal atrophy can result in conflicting data. Clarke and Lowry reported an absence of significant reductions in basal ganglionic NAA/Cr in MSA,¹⁶ precluding the use of NAA/Cr reductions in the striatum for differential diagnosis.¹⁶ Disease duration in their patients averaged 7.9 years.¹⁶ In contrast, mean disease duration in other reports showing significant NAA/Cr reductions in the striatum of MSA patients ranged from 3.2 to 4.5 years,¹¹⁻¹⁴ similar to the duration in our patients. Because, with longer duration, putaminal atrophy in patients with MSA-P becomes more severe, discrepancies could be explained by

differences in putaminal atrophy that can profoundly influence ¹H-MRS results. By avoiding this volume effect, MRS for the pontine base would provide a more accurate diagnostic marker.

Discriminating clearly between MSA-P and PD has long been a diagnostic problem from both therapeutic and prognostic viewpoints. Putaminal NAA/Cr reduction was significant in MSA-P patients compared with PD and control subjects, as previously reported.¹¹⁻¹⁴ However, as discussed above, the putaminal volume effect could influence the significance of putaminal NAA/Cr reduction, particularly in patients with advanced disease. Although brainstem and cerebellar involvement is an important and specific finding in differentiating MSA-P from PD,^{26, 32} the sensitivity of both clinical and MRI evaluations of these abnormalities is relatively low.^{7, 26} Based on our results, we believe that ¹H-MRS assessment of the pontine base would be of considerable value in the differential diagnosis between MSA-P and PD. However, combined ¹H-MRS study of the pontine base and putamen can provide a more sensitive differentiation between MSA-P and PD than a conventional single regional study, such as that of the putamen.

The cerebral hemisphere is involved more extensively in MSA than previously believed. Recently, Abe *et al* reported a significant decrease in NAA/Cr in MSA, involving Brodmann's areas 6, 8, and 46.¹⁴ Moreover, Spargo *et al*

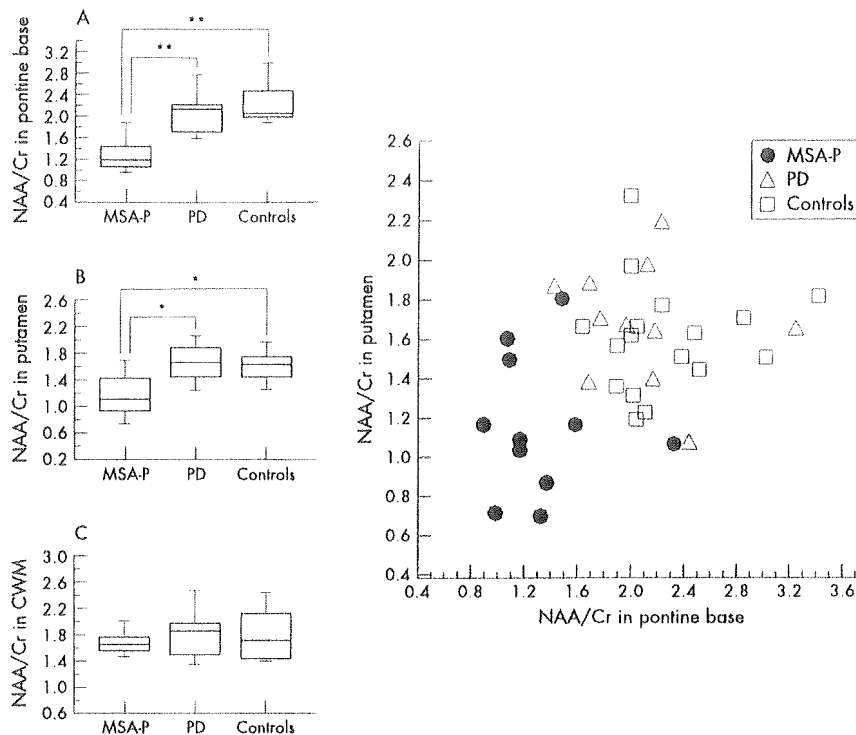


Figure 6 Box and whisker plot of the NAA/Cr ratio in the pontine base (A), putamen (B) and cerebral white matter (CWM, C) compared between MSA-P, PD, and controls. D is a scatter plot of the individual NAA/Cr data in the pontine base v putamen including MSA-P, PD, and control subjects. The scaled area corresponds to the mean \pm 2 SD of NAA/Cr in the pontine base and putamen of control subjects. * $p=0.002$, ** $p<0.0001$ by Scheffé's test, respectively. NAA, N-acetylaspartate; Cr, creatine; MSA-P, multiple system atrophy with parkinsonism predominant.

reported 18.7% and 21.4% neuronal loss in the primary and supplementary motor cortex, respectively.³³ In addition, the degree of atrophy in cerebral hemispheric areas varies between individuals, often becoming severe in long standing cases.³⁴ We found a mild overall reduction of NAA/Cr in CWM with a more significant NAA/Cr reduction in the subgroup with a longer duration of illness. This finding is in good agreement with previous ¹H-MRS reports and pathological observations.

Davie *et al*¹¹ reported a significant reduction of Cho/Cr ratio suggesting reduced membrane turnover in the lentiform nucleus in MSA, perhaps as result of cell loss. In the present study, Cho/Cr showed little change throughout the course of disease in the putamen, pontine base, and CWM, in agreement with other reports.^{12-14, 16} The relevance of this discrepancy is uncertain. One possible explanation is the difference of technical factors such as size of VOI and echo time. On the other hand, pathological study shows not only cell loss but also widely and variously distributed myelin degeneration in MSA brains that may increase the Cho.³⁵ Thus, heterogeneity of lesions in association with disease stage also may influence the Cho/Cr result. Further longitudinal studies and comparison of ¹H-MRS with histological findings will be needed to clarify the uncertainty as to the Cho/Cr ratio in MSA.

In conclusion, localised ¹H-MRS at 3.0 T in multiple regions showed widespread neuronal and axonal involvement in patients with MSA. NAA/Cr reduction in the pontine base provided a significant diagnostic marker for MSA irrespective of the disease form of MSA-P or MSA-C, disease duration, symptomatic manifestations, or MRI abnormalities. Moreover, combined ¹H-MRS study of the pontine base and putamen proved particularly effective in differentiating MSA from PD. We believe that ¹H-MRS would provide an early and accurate MSA diagnosis, an enhanced understanding of its pathogenetic mechanism, and the conclusiveness needed for future therapeutic trials.

Authors' affiliations

H Watanabe, M Katsuno, M Sugiura, K Hamada, Y Okada, M Hirayama, G Sobue, Department of Neurology, Nagoya University Graduate School of Medicine, Japan
H Fukatsu, T Ishigaki, Department of Radiology, Nagoya University Graduate School of Medicine, Japan

Competing interest: none declared

REFERENCES

- Graham JG, Oppenheimer DR. Orthostatic hypotension and nicotine sensitivity in a case of multiple system atrophy. *J Neurol Neurosurg Psychiatry* 1969;32:28-34.
- Quinn N. Multiple system atrophy—the nature of the beast. *J Neurol Neurosurg Psychiatry* 1989;52:78-89.
- Gilman S, Low PA, Quinn N, *et al*. Consensus statement on the diagnosis of multiple system atrophy. *J Neurol Sci* 1999;163:94-8.
- Sobue G, Terao S, Kachi T, *et al*. Somatic motor efferents in multiple system atrophy with autonomic failure: a clinico-pathological study. *J Neurol Sci* 1992;112:113-25.
- Wenning GK, Ben-Shlomo Y, Magalhes M, *et al*. Clinicopathological study of 35 cases of multiple system atrophy. *J Neurol Neurosurg Psychiatry* 1995;58:160-6.
- Lantos P. The definition of multiple system atrophy: A review of recent developments. *J Neuropathol Exp Neurol* 1998;57:1099-111.
- Watanabe H, Saito Y, Terao S, *et al*. Progression and prognosis in multiple system atrophy; an analysis of 230 Japanese patients. *Brain* 2002;125:1070-83.
- Ross B, Michaelis T. Clinical applications of magnetic resonance spectroscopy. *Magn Reson Q* 1994;10:191-247.
- Davie CA. The role of spectroscopy in parkinsonism. *Mov Disord* 1998;13:2-4.
- Rudkin TM, Arnold DL. Proton magnetic spectroscopy for the diagnosis and management of cerebral disorders. *Arch Neurol* 1999;56:919-26.
- Davie CA, Wenning GK, Barker GJ, *et al*. Differentiation of multiple system atrophy from idiopathic Parkinson's disease using proton magnetic resonance spectroscopy. *Ann Neurol* 1995;37:204-10.
- Federico F, Simone IL, Lucivero V, *et al*. Proton magnetic resonance spectroscopy in Parkinson's disease and atypical parkinsonian disorders. *Mov Disord* 1997;12:903-9.
- Federico F, Simone IL, Lucivero V, *et al*. Usefulness of proton magnetic resonance spectroscopy in differentiating parkinsonian syndromes. *Ital J Neurol Sci* 1999;20:223-9.
- Abe K, Terakawa H, Takashi M, *et al*. Proton magnetic resonance spectroscopy of patients with parkinsonism. *Brain Res Bull* 2000;52:589-95.

- 15 Terakawa H, Abe K, Watanabe Y, *et al*. Proton magnetic resonance spectroscopy (¹H MRS) in patients with sporadic cerebellar degeneration. *J Neuroimaging* 1999;9:72-7.
- 16 Clarke CE, Lowry M. Basal ganglia metabolite concentrations in idiopathic Parkinson's disease and multiple system atrophy measured by proton magnetic resonance spectroscopy. *Eur J Neurol* 2000;7:661-5.
- 17 Hu MTM, Simmons A, Glover A, *et al*. Proton magnetic resonance spectroscopy of the putamen in Parkinson's disease and multiple system atrophy. *Mov Disord* 1998;13:182.
- 18 Clarke CE, Lowry M. Systematic review of proton magnetic resonance spectroscopy of the striatum in parkinsonian syndromes. *Eur J Neurol* 2001;8:573-7.
- 19 Bomsdorf H, Helzel T, Kunz D, *et al*. Spectroscopy and imaging with a 4 Tesla whole-body MR system. *NMR Biomed* 1988;1:151-8.
- 20 Hetherington HP, Pan JW, Chu W-J, *et al*. Biological and clinical MRS at ultra-high field. *NMR Biomed* 1988;10:360-71.
- 21 Gruetter R, Weisdorf SA, Rajanayagan V, *et al*. Resolution improvements in vivo NMR spectra with increased magnetic field strength. *J Magn Reson* 1988;135:260-4.
- 22 Calne DB, Snow BJ, Lee C. Criteria for diagnosing Parkinson's disease. *Ann Neurol* 1992;32:S125-7.
- 23 Savoirdo M, Strada L, Giralti F, *et al*. Olivopontocerebellar atrophy: MR diagnosis and relationship to multiple system atrophy. *Radiology* 1990;174:693-6.
- 24 Kraft E, Schwarz J, Trenkwalder C, *et al*. The combination of hypointense and hyperintense signal changes on T2-weighted magnetic resonance imaging sequences: a specific marker of multiple system atrophy? *Arch Neurol* 1999;56:225-8.
- 25 Konagaya M, Sakai M, Matsuoka Y, *et al*. Pathological correlate of the shilike changes on MRI at the putaminal margin in multiple system atrophy. *J Neurol* 1999;246:142-3.
- 26 Schrag A, Good CD, Miszkil K, *et al*. Differentiation of atypical parkinsonian syndromes with routine MRI. *Neurology* 2000;54:697-02.
- 27 Moffett JR, Nambaodiri MAA, Cangro CB, *et al*. Immunohistochemical localization of N-acetylaspartate in rat brain. *Neuroreport* 1991;2:131-4.
- 28 Simmons ML, Frondoza CG, Coyle JT. Immunohistochemical localization of N-acetylaspartate with monoclonal antibodies. *Neuroscience* 1991;45:37-45.
- 29 Urenjak J, Williams SR, Gadian DG, *et al*. Specific expression of N-acetylaspartate in neurons, oligodendrocyte type-2 astrocyte progenitors, and immature oligodendrocyte in vitro. *J Neurochem* 1992;59:55-61.
- 30 Bhakoo KK, Pearce D. In vivo expression of N-acetylaspartate by oligodendrocytes: implications for proton magnetic resonance spectroscopy signal in vivo. *J Neurochem* 2000;74:254-62.
- 31 Bjartmar C, Battistuto J, Terada N, *et al*. N-acetylaspartate is an axon-specific marker of mature white matter in vivo: a biochemical and immunohistochemical study on the rat optic nerve. *Ann Neurol* 2002;51:51-8.
- 32 Litvan I, Goetz CG, Jankovic J, *et al*. What is accuracy of the clinical diagnosis of multiple system atrophy? *Arch Neurol* 1997;54:937-44.
- 33 Spargo E, Papp MI, Lantos PL. Decrease in neuronal density in the cerebral cortex in multiple system atrophy. *Eur J Neurol* 1996;13:450-6.
- 34 Konagaya M, Sakai M, Matsuoka Y, *et al*. Multiple system atrophy with remarkable frontal lobe atrophy. *Acta Neuropathol (Berl)* 1999;97:423-8.
- 35 Matsuo A, Akiguchi I, Lee GC, *et al*. Myelin degeneration in multiple system atrophy detected by unique antibodies. *Am J Pathol* 1998;153:671-6.



Have your say

eLetters

If you wish to comment on any article published in the *Journal of Neurology, Neurosurgery, and Psychiatry* you can send an eLetter using the eLetters link at the beginning of each article. Your response will be posted on *Journal of Neurology, Neurosurgery, and Psychiatry* online within a few days of receipt (subject to editorial screening).

www.jnnp.com

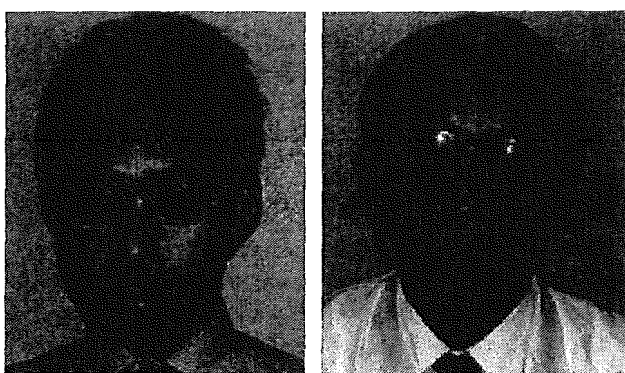
Masahisa Katsuno · Hiroaki Adachi ·
Fumiaki Tanaka · Gen Sobue

Spinal and bulbar muscular atrophy: ligand-dependent pathogenesis and therapeutic perspectives

Received: 29 September 2003 / Accepted: 13 January 2004 / Published online: 27 February 2004
© Springer-Verlag 2004

Abstract Spinal and bulbar muscular atrophy (SBMA) is a late-onset motor neuron disease characterized by proximal muscle atrophy, weakness, contraction fasciculations, and bulbar involvement. SBMA exclusively affects males, while females are usually asymptomatic. The molecular basis of SBMA is the expansion of a trinucleotide CAG repeat, which encodes the polyglutamine (polyQ) tract in the first exon of the androgen receptor (AR) gene. The histopathological hallmark is the presence

of nuclear inclusions containing mutant truncated ARs with expanded polyQ tracts in the residual motor neurons in the brainstem and spinal cord, as well as in some other visceral organs. The AR ligand, testosterone, accelerates AR dissociation from heat shock proteins and thus its nuclear translocation. Ligand-dependent nuclear accumulation of mutant ARs has been implicated in the pathogenesis of SBMA. Transgenic mice carrying the full-length human AR gene with an expanded polyQ tract demonstrate neuromuscular phenotypes, which are profound in males. Their SBMA-like phenotypes are rescued by castration, and aggravated by testosterone administration. Leuprorelin, an LHRH agonist that reduces testosterone release from the testis, inhibits nuclear accumulation of mutant ARs, resulting in the rescue of motor dysfunction in the male transgenic mice. However, flutamide, an androgen antagonist promoting nuclear translocation of the AR, yielded no therapeutic effect. The degradation and cleavage of the AR protein are also influenced by the ligand, contributing to the pathogenesis. Testosterone thus appears to be the key molecule in the pathogenesis of SBMA, as well as main therapeutic target of this disease.



MASAHISA KATSUNO is a Research Fellow in Neurology at Nagoya University Graduate School of Medicine, Nagoya, Japan. He received his M.D. and Ph.D. from Nagoya University. He has worked on therapeutic approaches for spinal and bulbar muscular atrophy.

GEN SOBUE is Professor of Neurology at Nagoya University Graduate School of Medicine, Nagoya, Japan. He received his M.D. and Ph.D. from Nagoya University, and has worked at the University of Pennsylvania School of Medicine and Aichi Medical University. His research interests include the development of therapies for neurodegenerative diseases and peripheral neuropathies.

Keywords Spinal and bulbar muscular atrophy · Polyglutamine · Androgen receptor · Ligand · Testosterone · Heat shock protein

Introduction

More than a hundred years have elapsed since the first description of spinal and bulbar muscular atrophy (SBMA) [1, 2]. Early case reports [3, 4, 5, 6, 7, 8] were followed by the clinical and genetic description of 11 cases from two families by Kennedy and colleagues [9], which established the clinical entity of SBMA. Since the discovery of abnormal CAG triplet expansion in the androgen receptor (AR) gene as the cause of SBMA [10], molecular biological approaches have been undertaken to elucidate the pathogenesis of the disease and develop

M. Katsuno · H. Adachi · F. Tanaka · G. Sobue (✉)
Department of Neurology,
Nagoya University Graduate School of Medicine,
65 Tsurumai-cho, Showa-ku, 466-8550 Nagoya, Japan
e-mail: sobueg@med.nagoya-u.ac.jp
Tel.: +81-52-7442385, Fax: +81-52-7442384

approaches for its treatment. Here we review the research findings from which the ligand-dependent pathophysiology of SBMA has emerged, and discuss its therapeutic approaches.

Clinical features of SBMA

SBMA, also known as Kennedy's disease, is an inherited motor neuron disease characterized by adult-onset proximal muscle atrophy, weakness, fasciculations, and bulbar involvement [9, 11]. Fasciculations often manifest upon muscle contraction, and have been described as contraction fasciculations. The onset of weakness is usually between 30 and 50 years, but is often preceded by nonspecific symptoms such as tremor, muscle cramps and fatigue [12, 13]. Deep tendon reflex is diminished or absent, with no pathological reflex. Sensory involvement is largely restricted to that of vibration, which is affected distally in the legs [11]. Male patients occasionally demonstrate signs of androgen insensitivity such as gynecomastia, testicular atrophy, erectile dysfunction and decreased fertility [14, 15, 16], and some of these symptoms may be detected before the onset of motor symptoms. Endocrinological examinations frequently reveal partial androgen resistance with an elevated serum testosterone level [17]. Examination by electromyogram shows neurogenic abnormalities, and distal motor latencies are often prolonged in nerve conduction studies. Both the sensory nerve action potential and sensory evoked potential are reduced or absent [18, 19]. Serum creatine kinase levels are elevated in the majority of patients. Hyperlipidemia, liver dysfunction and glucose intolerance are also detected in some patients [12, 20]. SBMA exclusively affects males, and thus has been reported as an X-linked hereditary disease. The prevalence of SBMA has been estimated 1 in 40,000 in areas with where the diagnosis is efficient [21], although considerable numbers of patients may have been under-diagnosed [22, 23]. Profound facial fasciculations, bulbar signs, gynecomastia, and sensory disturbance are the main clinical features distinguishing SBMA from other motor neuron diseases, although genetic analysis is indispensable for diagnosis. Female patients are usually asymptomatic, but some express subclinical phenotypes including high amplitude motor unit potentials on electromyography [24, 25].

In the histopathology of SBMA, lower motor neurons are markedly depleted through all spinal segments and in the brainstem motor nuclei except the third, fourth and sixth cranial nerves [11, 26]. The number of nerve fibers is reduced in the ventral spinal nerve root, reflecting motor neuronopathy. Sensory neurons in the dorsal root ganglia are less severely affected, and the large myelinated fibers demonstrate a distally accentuated sensory axonopathy in the peripheral nervous system [27]. Neurons in the Onufrowicz nuclei, intermediolateral columns and Clarke's columns of the spinal cord are generally well preserved. Muscle histopathology shows both neurogenic and myogenic findings; there are groups of atrophic fibers

with a number of small angular fibers, fiber type grouping, and clumps of pyknotic nuclei as well as variability in fiber size, hypertrophic fibers, scattered basophilic regenerating fibers and central nuclei.

The progression of SBMA is usually slow, but life-threatening respiratory tract infection often occurs in the advanced stage of the disease, resulting in early death in some patients [13]. No specific treatment for SBMA has been established. Testosterone has been used in some patients, although it has no effects on the progression of the disease [28, 29, 30].

Molecular pathogenesis of SBMA

The molecular basis of SBMA is the expansion of a trinucleotide CAG repeat, which encodes the polyglutamine (polyQ) tract, in the first exon of the AR gene [10] (Fig. 1). The CAG repeat within AR ranges in size from 11 to 35 repeats in normal subjects, but from 40 to 62 in SBMA patients [10, 21, 31]. Multiple founder effects have been reported in Japan, Europe and Australia [31, 32]. Expanded polyQ tracts have been found to cause several neurodegenerative diseases including SBMA, Huntington's disease (HD), several forms of spinocerebellar ataxia, and dentatorubral and pallidolusian atrophy (DRPLA) [33, 34, 35]. These disorders, known as polyQ diseases, share salient clinical features such as anticipation [36], somatic mosaicism [37], and selective neuronal and non-neuronal involvement despite widespread expression of the mutant gene [38]. There is also an inverse correlation between the CAG repeat size and the age at onset, or the disease severity adjusted by age at examination in SBMA [36, 39], as well as in other polyQ diseases [33, 40]. These observations suggest that common mechanisms underlie the pathogenesis of polyQ diseases, although the nature of each causative protein is discrete apart from the existence of the polyglutamine stretch.

A striking pathological hallmark of most polyQ diseases is the presence of nuclear inclusions (NIs), which have been considered relevant to the pathophysiology [33]. In SBMA patients, NIs containing the mutant,

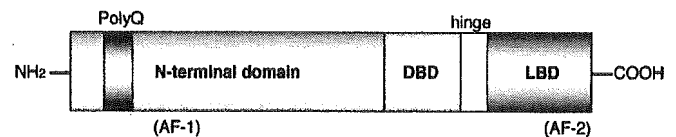


Fig. 1 Structure of the androgen receptor (AR) protein. The AR, a ligand-dependent transcriptional factor, is a member of the steroid/thyroid hormone receptor family. The AR protein consists of three major domains: an N-terminal transactivating domain, a DNA-binding domain, and a ligand-binding domain. The polyglutamine tract is located in the N-terminal domain, which possesses the major transactivating function (*AF-1*). The DNA binding domain (*DBD*) contains zinc finger structures, facilitating AR binding to DNA. The ligand binding domain (*LBD*) in the C-terminus also contains weak transactivating function (*AF-2*)

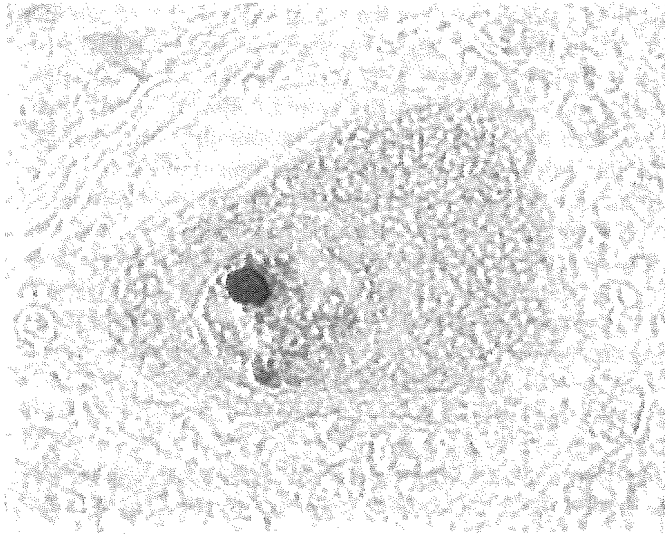


Fig. 2 Nuclear inclusion of spinal and bulbar muscular atrophy (SBMA). A residual motor neuron in the lumbar anterior horn shows a nuclear inclusion detected by an anti-polyglutamine antibody

truncated AR are detected in the residual motor neurons in the brainstem and spinal cord [41] (Fig. 2) as well as in the skin, testis and some other visceral organs [42]. These inclusions have similar epitope features detectable by antibodies that recognize a small portion of the N-terminus of the AR protein only, and they are ubiquitinated. Although considerable controversy surrounds the importance of NIs in the pathophysiology of the polyQ diseases [43], several studies have implied that the nuclear localization of the mutant protein is essential for inducing neuronal cell dysfunction and degeneration in the majority of polyQ diseases [34]. This hypothesis is supported by the fact that several transcriptional regulatory proteins are sequestered into NIs [44, 45].

SBMA is unique among polyQ diseases in that the mutant protein, the AR, has a specific ligand, testosterone, and this ligand alters the subcellular localization of the protein by favoring its nuclear uptake. The AR is normally confined to a multi-heteromeric inactive complex in the cell cytoplasm, and translocates into the nucleus in a ligand-dependent manner [46]. This intracellular trafficking of AR and other ligand-related mechanisms appear to play important roles in the pathogenesis of SBMA.

Ligand effects in a mouse model of SBMA

In order to investigate ligand effects in SBMA, we generated transgenic mice expressing the full-length human AR containing either 24 or 97 CAG repeats under the control of a cytomegalovirus enhancer and a chicken β -actin promoter [47]. This model recapitulated not only the neurological disorder, but also the phenotypic differences with gender, which is a specific feature of SBMA.

The lines with 97 CAG repeats (AR-97Q) exhibited progressive motor impairment, although no lines with 24 CAG repeats showed any phenotypes. All symptomatic lines showed small body size, short lifespan, progressive muscle atrophy and weakness, as well as reduced cage activity, all of which were pronounced and markedly accelerated in the male AR-97Q mice, but were either not observed, or far less severe, in the female AR-97Q mice, regardless of the line. The onset of motor impairment detected by the rotarod task was between 8 and 9 weeks of age in the male AR-97Q mice, and at 16 weeks or more in the females. The 50% mortality ranged from 66 to 132 days in the male AR-97Q mice, whereas the mortality of the females remained only 10–30% at more than 210 days. Western blot analysis revealed the transgenic protein smearing from the top of the gel, indicating the presence of insoluble AR fragments, in tissues such as the spinal cord, cerebrum, heart, muscle and pancreas. Although the male AR-97Q mice had more smearing protein than their female counterparts, the female AR-97Q mice had more monomeric AR protein. The nuclear fraction contained the most of smearing mutant AR protein. Diffuse nuclear staining and less frequent NIs detected by 1C2, an antibody specifically recognizing the expanded polyQ, were demonstrated in the neurons of the spinal cord, cerebrum, cerebellum, brainstem and dorsal root ganglia as well as non-neuronal tissue such as the heart, muscle and pancreas. Male AR-97Q mice showed markedly more abundant diffuse nuclear staining and NIs than females, in agreement with the symptomatic and Western blot profile differences with gender. Despite the profound sexual differences of mutant AR protein expression, there was no significant difference in the expression of the transgene mRNA between the male and female AR-97Q mice. These observations indicate that the testosterone level plays an important role in the gender-specific differences in the phenotypes, especially in post-transcriptional regulation of the mutant AR. Gender-specific phenotypes have also been demonstrated in another transgenic mouse model of SBMA carrying the full-length AR with 120 CAG repeats driven by a cytomegalovirus promoter [48].

The dramatic sexual difference of phenotypes led us to trial hormonal interventions in our mouse model. First, we castrated male AR-97Q mice in order to decrease their testosterone level. Castrated males showed profound improvement of their symptoms, histopathological findings, and nuclear localization of the mutant AR compared with sham-operated males. The body weight, motor function, and lifespan of these mice were significantly improved by castration. Western blot analysis and histopathology revealed diminished nuclear accumulation of mutant AR in the castrated males compared with the sham-operated males. Next, we administered testosterone to female AR-97Q mice. In contrast to castration of the male mice, testosterone caused a significant aggravation of symptoms, histopathological features, and nuclear localization of the mutant AR in female mice. Since the nuclear translocation of AR is testosterone-dependent,

testosterone appears to show toxic effects in the female AR-97Q mice by accelerating nuclear translocation of the mutant AR. Hence, castration of the males prevented the nuclear localization of the mutant AR by reducing the testosterone level. Nuclear localization of the mutant protein with an expanded polyQ tract is likely to be important in inducing neuronal cell dysfunction and degeneration in the majority of the polyQ diseases. Addition of a nuclear export signal to the mutant huntingtin protein eliminates aggregate formation and cell death in cell models of HD [49, 50], whereas a nuclear localization signal has the opposite effect [50]. When its nuclear localization signal is mutated, atxaxin-1, the causative protein of SCA-1, is distributed in the cytoplasm and does not cause any neurological disorders in SCA1 transgenic mice [43]. Addition of a nuclear export signal to the mouse Hprt protein containing expanded polyQ reduces NIs and delays the onset of behavioral abnormalities [51]. These findings suggest that reduction in the testosterone level improved phenotypic expression by preventing nuclear localization of the mutant AR. In support of this hypothesis, the ligand-dependent neurodegeneration has also been revealed in a fruit fly model of SBMA [52]. Alternatively, castration may enhance the protective effects of heat shock proteins, which are normally associated with the AR and dissociate upon ligand binding. Although ligand-induced neuronal dysfunction is apparent in the mouse model, testosterone administration does not worsen the symptoms of SBMA patients in preliminary clinical trials [28, 29]. This inconsistency may be explained by several reasons. The treatment duration may not be long enough to show its negative effects on disease progression. The negative effect may be saturated by the endogenous level of testosterone. The anabolic effects of androgens on the muscle may attenuate the motor symptoms induced by anterior horn cell degeneration in SBMA.

Successful treatment of AR-97Q mice by castration inspired us to trial testosterone blockade therapies, using a LHRH analogue and an AR antagonist used in the treatment of prostate cancer [53]. AR-97Q mice treated with leuporelin, a LHRH analogue which reduces testosterone release from the testis, showed a marked amelioration of symptoms, histopathological findings, and nuclear localization of the mutant AR compared with vehicle-treated mice (Fig. 3). Leuporelin initially increased the serum testosterone level by upregulating the LHRH receptor, but this effect was subsequently reduced to undetectable levels. Androgen blockade effects were also confirmed by reduced weights of the prostate and the seminal vesicle. The leuporelin-treated AR-97Q mice showed significant improvements in lifespan, muscle atrophy and reduced body size as well as motor impairment as assessed by the rotarod task and cage activity. Although the negative effect on fertility was mitigated by reducing the dosage, the therapeutic effects on neuromuscular phenotypes were insufficient at a lower dose of leuporelin. In the Western blot analysis and anti-polyglutamine immunostaining, the leuporelin-treated male

AR-97Q mice had markedly diminished levels of mutant AR in the nucleus, suggesting that leuporelin successfully reduced nuclear AR accumulation. Testosterone, which was given from 13 weeks of age, markedly aggravated the neurological symptoms and pathological findings of the leuporelin-treated male AR-97Q mice. Leuporelin prevents testicular testosterone production by down-regulating LHRH receptors in the pituitary, and has extensively been used as medical castration in the therapy of prostate cancer. Leuporelin appears to improve SBMA-related neuronal dysfunction by preventing ligand-dependent nuclear translocation of the mutant AR in the same way as castration. Given its minimal invasiveness and established safety, leuporelin is likely to be a promising therapeutic agent for SBMA. Upon clinical trials, however, the patient's desire for fertility should be taken into account, and the appropriate therapeutic dose carefully determined.

Leuporelin-treated AR-97Q mice showed deterioration in their body weights and rotarod task performance from the age of 8–9 weeks, when serum testosterone initially increased through the agonistic effect of leuporelin. This change was transient and followed by a sustained amelioration together with consequent suppression of testosterone production. The footprint analyses also revealed a temporary exacerbation of motor impairment. Immunostaining of tail specimens, sampled from the same individual mouse, demonstrated an increase in the number of the muscle fibers with nuclear 1C2 staining after 4 weeks of leuporelin administration, although this 1C2 staining was diminished after another 4 weeks of treatment. Reversibility of polyQ pathogenesis has also been demonstrated by turning off gene expression in an inducible mouse model of HD [54]. Our results, however, indicate that preventing nuclear translocation of the mutant AR is enough to reverse both the symptomatic and pathological phenotypes in our AR-97Q mice. Since the pathophysiology of AR-97Q mice is neuronal dysfunction without neuronal cell loss [47], our results indicate that polyQ pathogenesis is reversible at least in its dysfunctional stage. We need to determine the early dysfunctional period in human polyQ diseases.

By contrast, flutamide, an AR antagonist, did not ameliorate the symptoms, pathological features, or nuclear localization of the mutant AR in the male AR-97Q mice, although there was no significant difference between flutamide and leuporelin in terms of androgen blockade. Flutamide, the first androgen antagonist discovered, has a highly specific affinity for the AR, and competes with testosterone for binding to the receptor. It has been used for the treatment of prostate cancer, usually in association with an LHRH agonist, in order to block the action of adrenal testosterone. Although flutamide suppresses androgen-dependent transactivation, it does not reduce the plasma levels of testosterone. Furthermore, flutamide does not inhibit, but may even facilitate, the nuclear translocation of the AR [55, 56]. Flutamide also promotes nuclear translocation of mutant ARs containing expanded polyQ tracts in both cell and fly models of